UCL
Université catholique de Louvain
Faculté des Sciences Appliquées

NUMERICAL STUDY OF FREE SURFACE NEWTONIAN AND VISCOELASTIC FLOWS

R. Sizaire

Thèse présentée en vue
de l'obtention du grade de
Docteur en Sciences Appliquées

Promoteur:
Dr. V. Legat

Janvier 1998

THIS PAGE IS INTENTIONALLY LEFT BLANK

The most exciting phrase to hear in science, the one that heralds new discoveries, is not "Eureka!" (I found it!) but "That's funny..."

Isaac Asimov

THIS PAGE IS INTENTIONALLY LEFT BLANK

Acknowledgements

At the end of four years of research, I would like to thank all people that have contributed to the realization of my thesis.

Professor Marcel Crochet initiated my research on encapsulation and was my supervisor during three years. I also thank him for his confidence, and also for providing an excellent environment for research in MEMA.

Next, all my thanks go to my second supervisor, Doctor Vincent Legat. His availability, and the numerous interesting dicussions I have got with him, have been for me powerful stimulants during three years.

I also would like to thank Professor Roland Keunings for numerous advises. He gave me the opportunity to take advantage of his experience.

I also thank Professor Paul Van Dooren and Professor Ken Walters for reading the preliminary version of this text. Many improvements were brought to the final version thanks to their comments and suggestions. Finally, I Thank Professor Pierre Wauters to accept to preside the jury of this thesis.

During the four years I have spent in the Euler building, I have met many people. Most of them are more than colleagues for me. I thank them all for the excellent time we had together. My gratitude also goes to Edmond, Guido, Victor, Edward, Michèle and Brigitte for their help and availability.

Finally I want to thank my whist partners who have done so much to improve my skills in playing cards.

THIS PAGE IS INTENTIONALLY LEFT BLANK

To my parents

THIS PAGE IS INTENTIONALLY LEFT BLANK

Preface

Many problems are so complex that it is impossible to study them analytically. For such problems, the use of numerical methods may be an interesting complement to experimental investigations. During the last years, the development of computational software has gained an increasing interest in industry. Indeed, the use of those softwares by engineers may lead to a dramatic reduction of time and cost in the development of new processes.

For example, for many years, the design of a die has been a work in which the intuition of the engineer has played a major role. In many cases however, intuition was not sufficient to design the die, and several attempts had to be done to obtain an acceptable device. But, the construction of a die is an expensive operation, and the lack of trustworthy methods to predict the corresponding extrudate shape has often led to wasted time and money [Leg92]. In the years to come, we may expect an increase in the use of computational software related to the development of powerful and cheap computers.

Besides the development of computer simulation, research is done to better understand the behaviour of complex fluids such as polymer solutions, polymer melts, paints, rubbers,... Those studies are subjects of the science called "rheology". That science has led to the development of constitutive equations relating stresses to deformations inside the material. But the use of those models often gives rise to numerical difficulties. This is often the case for viscoelastic models. Special numerical techniques have been (and are still being) developed to deal with the computation of such viscoelastic flows.

But the results of rheological science and numerical developments are not sufficient to give a complete solution to most of the problems of polymer processing. Many problems are so complicated that a pragmatic approach must be adopted. For example, the results of experimental observations and analytical modelling may help the engineer to identify the most relevant parameters of the process, and develop a simplified model reproducing most phenomena of interest of the process.

This text is divided in two parts:

- At the beginning of this research, we thought that encapsulation was the result of the development of an interfacial instability. This has led us to investigate the stability of multilayer flows. Chapter 2 is devoted to that study. In particular, we present the results of time-dependent numerical

calculations of interfacial perturbations growing into the nonlinear domain. We show that it is possible to reproduce nonlinear flow regimes observed experimentally like the bamboo waves in core-annular flows. Those results are obtained with transient calculations of two-dimensional Newtonian flows. But three-dimensional transient calculations are needed to reproduce transient development of instabilities towards encapsulation. The computational cost of those calculations is prohibitive. Therefore, we investigate in chapter 3 another possible explanation of the encapsulation: we study the influence of second normal stress difference on the phenomenon. The advantage of that explanation is that it may be checked with time-independent calculations. Finally, our calculated results are compared to experimental observations for a realistic case of coextrusion.

- In chapter 4, we present the results of a numerical study of a filament stretching device. We determine the conditions under which the device produces trustworthy results and we propose an improved estimate of the extensional viscosity. The effects of material parameters and of the initial gap between the plates are investigated too. The calculations of chapter 4 have been done with FENE-CR model. However, some experimental observations cannot be reproduced with the FENE-CR model. In chapter 5, we investigate the influence of the macromolecular structure on the rheological behaviour of polymer solutions in uniaxial extensional flows. We propose a multimode model, and we show that it is suitable to reproduce many experimental results.

Parts I and II are independent. Consequently, we introduce and conclude them separately. In chapter 1, we present the theoretical background necessary to understand the other chapters of the text.

Several results presented in this text have led to publications. Most results given in chapter 4 have been first presented in

- R. Sizaire and V. Legat. Finite element simulation of a filament stretching rheometer. *Journal of Non-Newtonian Fluid Mechanics*, 71:89–107, 1997.

The study of the influence of the macromolecular structure on the behaviour of polymer solutions in extensional flows (chapter 5) will be published in

- R. Sizaire, G. Lielens, I. Jaumain, R. Keunings, and V. Legat. Influence of non-linearity and dispersity on the behaviour of viscoelastic fluids in rheometrical extensional flows. *to be submitted to the Journal of Non-Newtonian Fluid Mechanics*, 1998.

Finally, the results of our investigation of the influence of second normal stress difference on the encapsulation (chapter 3) will be given in

- R. Sizaire and V. Legat. Calculation of 3D encapsulation flows with the finite element method. *to be submitted to the Journal of Rheology*, 1998.

Contents

Glossary

In this glossary, we summarize the notations used in this text. We first present the abbreviations, and then the general notations. Unfortunately, notations may vary from chapter to chapter. This is mainly related to the fact that several subjects have been investigated, and we try to use the standard notations in the text. Therefore, some of the notations are introduced or redefined in sections corresponding to the chapters.

Abbreviations

AVSS	adaptive viscous split stress formulation	17
BW	bamboo waves	68
CAF	core-annular flow	68
DBW	disturbed bamboo waves	68
DCAF	disturbed core-annular flow	68
DEVSS	discrete elastic viscous split stress formulation	17
EVSS	elastic viscous split stress formulation	17
FENE-CR	Chilcott and Rallison closure of FENE model	13
FENE-PM	closure of Wedgewood et al.	153
FENE-P	Peterlin closure of FENE model	13
FENE	finitely extensible nonlinear elastic (dumbbell)	12
LBB	Ladyzhenskaya, Babuska and Brezzi condition of stability	15
LDPE	low density polyethylene	90
MIX	MIX formulation	15
PCJ	Preziosi, Chen and Joseph	62
PS	polystyrene	90
PTT	Phan-Thien-Tanner model	8
SAM	Spiegelberg, Ables and McKinley	138
SUPG	streamline upwind Petrov-Galerkin formulation	18
SU	streamline upwind formulation	18

General notations

$\boldsymbol{A}$	configuration tensor	13

α_{G}	one of the parameters of Giesekus model 8
Bo	Bond number 133
Ca	capillary number 133
C_{p}	heat capacity 2
D/Dt	material derivative 1
De	Deborah number 14
Δt	time step 44
$\boldsymbol{\delta}$	unit tensor 99
:	scalar product of two tensors 2
$\boldsymbol{D}$	rate of deformation tensor 3
$\dot{\epsilon}$	extension rate 4
ϵ_{PTT}	one of the parameters of PTT model 8
$\overline{\eta}^{+}$	transient extensional viscosity 133
η_E	extensional viscosity in regime 4
η_N	Newtonian part of the shear viscosity 7
η	shear viscosity 3
η_V	viscoelastic part of the shear viscosity 7
$\boldsymbol{F}^b$	brownian forces on a dumbbell 11
$\boldsymbol{F}^c$	connector force between the beads 11
F	Froude number 32
$\boldsymbol{F}^h$	hydrodynamic drag forces on a dumbbell 11
4×4	4×4 element of Marchal and Crochet 16
$\boldsymbol{f}$	volumic force 2
Γ	boundary of the computational domain Ω 191
$\dot{\gamma}$	velocity gradient 3
γ	surface tension 22
g	magnitude of dimensionless gravity 72
H	stiffness factor for the spring 12
$h(x,t)$	displacement of the interface 24
$\boldsymbol{I}$	unit tensor 2
k	Boltzmann constant 11
k_{slip}	slip coefficient 84
k	thermal conductivity 2
λ	relaxation time 6
λ_R	retardation time 7
$< B >$	average value of B 11
L^2	extensibility of the dumbbells 13
μ	viscosity 32
$\nabla\cdot$	divergence of a vectorial field 1
∇^2	Laplacian operator 19
$\boldsymbol{\nabla}\cdot$	divergence of a tensorial field 2
$\boldsymbol{\nabla}$	gradient of a scalar function 2
n	number of dumbbells per unit of volume 11
N_1	first normal stress difference 4
$\boldsymbol{n}$	outward unit normal vector 15
N_2	second normal stress difference 4

Stability of multilayer Newtonian flows

A	amplitude of the perturbation ... 46
A_{init}	initial amplitude of the perturbation ... 43
αc_i	growth rate of the perturbation ... 33
α	wavenumber of the perturbation ... 33
A_p	amplitude of harmonic p ... 46
a	radius ratio ... 62
B	amplitude of the perturbation on flow rates ... 55
c	eigenvalue of the problem ... 33
$\chi(y)$	eigenfunction in Orr-Sommerfeld equations (lower layer) ... 34
$\Delta t_{\text{perturb}}$	duration of perturbation on the flow rates ... 55
f_n	pushing force on the inlet section ... 42
$\boldsymbol{G}$	dimensionless gravity ... 32
$\boldsymbol{g}$	gravity ... 32
H	height of the mesh for axisymmetric calculations ... 70
h	hold-up ratio ... 71
J^*	dimensionless surface tension of Preziosi, Chen and Joseph ... 62
L	length of the computational domain ... 40
m	viscosity ratio ... 32
n	thickness ratio ... 32
ω	frequency of the perturbation on the flow rates ... 55
$\phi(y)$	eigenfunction in Orr-Sommerfeld equations (upper layer) ... 33
S	dimensionless surface tension ... 32, 63
$\hat{u}$, $\hat{v}$, $\hat{p}$	perturbed quantities on u, v and p ... 33
u', v', p'	perturbations on u, v and p ... 33
V_{o}	superficial velocities of oil ... 68
V_{w}	superficial velocities of water ... 68
ζ	density ratio ... 32

Numerical calculations of encapsulation

$\boldsymbol{\delta}_{\text{II}}$	projection tensor onto the local tangent plane ... 99
$\boldsymbol{F}_l$	contact force along the contact line ... 100
F_r	radial component of the contact force ... 100
$\boldsymbol{F}_t$	tangential component of the contact force ... 99
κ	parameter of the Bird-Carreau law for ψ_2 ... 94
λ_{N}	parameter of the Bird-Carreau viscosity law ... 92
m	power law index for ψ_2 ... 94
n	power-law index for the Bird-Carreau viscosity law ... 92
$\boldsymbol{r}$	radial vector ... 100
u_n	normal component of the velocity ... 99
u_t	tangential component of the velocity ... 99

The filament stretching device

$\dot{\epsilon}_{\mathrm{pl}}$	"plate" estimate of the strain rate 130
$\dot{\epsilon}_{\mathrm{rad}}$	radial estimate of the strain rate 142
ϵ_{pl}	"plate" estimate of the Hencky strain 130
ϵ_{rad}	radial estimate of the Hencky strain 142
$\overline{\eta}^{+}_{\mathrm{pl}}$	plate estimate of extensional viscosity 142
$\overline{\eta}^{+}_{\mathrm{rad}}$	radial estimate of extensional viscosity 143
F	force measured on the lower plate 141
L	length of the filament 130
L_0	initial length of the filament 130
R	minimum radius of the filament 130
R_0	initial radius of the sample 130
τ	tension in the filament 142

Molecular effects in extensional flows

$\boldsymbol{a}_i$	new dimensionless configuration tensor 168
$\boldsymbol{A}_{\mathrm{max}}$	configuration tensor of the largest extensibility mode 164
Δt_{stop}	time necessary to stop the upper plate 160
$\dot{\epsilon}_{\mathrm{up}}$	strain rate during elongation 160
$\boldsymbol{\kappa}^{\dagger}$	transposition of tensor $\boldsymbol{\kappa}$ 157
$\boldsymbol{\kappa}$	rate of deformation tensor 157
L^i_2	extensibility parameter of mode i 157
L^2_{max}	maximum extensibility parameter 157
L^2_{min}	minimum extensibility parameter 157
$\boldsymbol{Q}_j$	vector connecting two consecutive beads 156
Q_0	equilibrium length for the springs in the chain model 156
t_{stop}	time at which the upper plate is stopped 160
we	weighting parameter for the distribution function 157

Chapter 1

Theoretical background

The mathematical modelling of flows is described by the theory of continuum mechanics. The governing equations consist of conservation equations and constitutive equations. The equations are derived from the principle of conservation of mass, the principle of balance of linear momentum, and the principle of balance of energy. Constitutive equations are relating the stresses in the fluid to the deformation history.

Whereas conservation equations apply whatever the material studied, the constitutive equations depend from the material. In the section devoted to constitutive equations, we introduce the generalized Newtonian model, and the differential viscoelastic models.

The conservation and constitutive equations are used to calculate flows in complex geometries. For such problems, it is generally not possible to calculate an analytical solution of the governing equations. We use finite elements to solve that kind of problems. The principles of the finite elements, and their application to the calculation of viscoelastic flows is shortly presented. We also describe how solutions on moving domains are calculated.

Of course this chapter is mainly a literature overview. Most information presented here has been found in [Mac94, CAD+95a, Pur96, BHAC77, BCAH87, Lar88, Bod94, Leg92, War96]. The preceding list is not exhaustive.

1.1 Conservation equations

1.1.1 Conservation of mass

Let $\rho(\boldsymbol{x}, t)$, $\boldsymbol{v}(\boldsymbol{x}, t)$ be respectively the volumic mass and the velocity defined at a material point of coordinates $\boldsymbol{x}$ and at time t. The principle of conservation of mass is expressed as

$$\frac{D\rho}{Dt} + \rho \nabla \cdot \boldsymbol{v} = 0,$$

where D/Dt denotes the material derivative and $\nabla\cdot$ is the divergence. Usually, most liquids may be considered as incompressible. This equation is usually called

"continuity equation". If the fluid is incompressible, the density is a constant, and the continuity equation reduces to

$$\nabla \cdot \boldsymbol{v} = 0. \tag{1.1}$$

1.1.2 Conservation of linear momentum

The equation of motion arises from the principle of balance of linear momentum. It is written as

$$\rho \frac{D\boldsymbol{v}}{Dt} = \boldsymbol{\nabla} \cdot \boldsymbol{\sigma} + \boldsymbol{f}, \tag{1.2}$$

in which $\boldsymbol{f}$ is the resultant of volumetric forces, and $\boldsymbol{\sigma}(\boldsymbol{x}, t)$ is the Cauchy stress tensor.

1.1.3 Conservation of angular momentum

The balance of angular momentum requires the Cauchy stress tensor to be symmetric:

$$\boldsymbol{\sigma} = \boldsymbol{\sigma}^{\mathrm{T}}. \tag{1.3}$$

1.1.4 Conservation of energy

The energy equation balances the internal energy of the fluid U, the viscous dissipation $\boldsymbol{\sigma} : \boldsymbol{\nabla v}$, the energy produced in the fluid r (for example by a chemical reaction), and the energy transported by conduction $\boldsymbol{q}$:

$$\rho \frac{DU}{Dt} = \boldsymbol{\sigma} : \boldsymbol{\nabla v} + r - \nabla \cdot \boldsymbol{q}. \tag{1.4}$$

If we only consider the thermal energy (i.e. the energy corresponding to the temperature of the fluid), and assuming that the conduction satisfies the Fourier law $\boldsymbol{q} = -k\boldsymbol{\nabla} T$, equation (1.4) becomes

$$\rho C_{\mathrm{p}} \frac{DT}{Dt} = \nabla \cdot (k \boldsymbol{\nabla} T) + \boldsymbol{\sigma} : \boldsymbol{\nabla v} + r. \tag{1.5}$$

In equation (1.5), we have introduced the temperature T, the heat capacity C_{p}, and the thermal conductivity k.

1.2 Constitutive equations

The Cauchy stress tensor may be separated into two contributions:

$$\boldsymbol{\sigma} = -p\boldsymbol{I} + \boldsymbol{T},$$

in which p is the pressure, $\boldsymbol{I}$ is the unit tensor and $\boldsymbol{T}$ is the extra-stress tensor.

The conservation equations presented in section 1.1 are not sufficient to determine the unknowns corresponding to the flow. Constitutive equations are introduced to relate the history of a material point to its extra-stress tensor $\boldsymbol{T}$.

1.2.1 Newtonian fluids

For an incompressible Newtonian viscous fluid, the extra-stress tensor is given by

$$\boldsymbol{T} = 2\eta \boldsymbol{D}, \tag{1.6}$$

in which η is the constant shear viscosity, and $\boldsymbol{D}$ is the rate of deformation tensor

$$\boldsymbol{D} = \frac{\boldsymbol{\nabla v} + \boldsymbol{\nabla v}^{\mathrm{T}}}{2}.$$

Most small molecule liquids such as water, oil, gases obey the constitutive law (1.6). But other liquids have a more complex behaviour. The study of those liquids is the subject of the science called "rheology".

1.2.2 Non-Newtonian fluids

The peculiar properties of non-Newtonian fluids may be observed in rheometrical flows. We present here the main non-Newtonian effects in steady simple shear flow, and in uniaxial extensional flow.

In order to simplify the following expressions, we introduce here the notations for the components of velocity and coordinate fields: $\boldsymbol{v} = (u, v, w)^{\mathrm{T}}$, $\boldsymbol{x} = (x, y, z)^{\mathrm{T}}$.

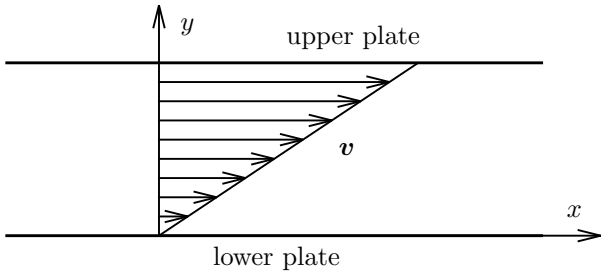

Figure 1.1: *Steady Couette flow.*

In steady simple shear flow (Figure 1.1), the velocity components are given by

$$u = \dot{\gamma} y, \qquad v = w = 0, \tag{1.7}$$

in which $\dot{\gamma}$ is the constant velocity gradient. The shear rate $\dot{\gamma}$ may also be defined for complex flows. It is related to the second invariant $\boldsymbol{D} : \boldsymbol{D}$ of the rate of deformation tensor $\boldsymbol{D}$ by

$$\dot{\gamma} = \sqrt{2\boldsymbol{D} : \boldsymbol{D}}.$$

Replacing the velocity field (1.7) in the constitutive relation (1.6), we find a Cauchy stress tensor, the components of which satisfy the relations

$$\sigma_{xy} = \eta\dot{\gamma}, \qquad \sigma_{xx} - \sigma_{yy} = 0, \qquad \sigma_{yy} - \sigma_{zz} = 0. \tag{1.8}$$

In the case of non-Newtonian fluids, the measurements will give other results:

$$\sigma_{xy} = \eta(\dot{\gamma})\dot{\gamma}, \qquad \sigma_{xx} - \sigma_{yy} = N_1(\dot{\gamma}), \qquad \sigma_{yy} - \sigma_{zz} = N_2(\dot{\gamma}). \tag{1.9}$$

Three differences arise from the comparison of the Newtonian predictions (1.8) and the non-Newtonian observations (1.9):

- The measured shear viscosity $\eta(\dot{\gamma})$ depends on the shear rate $\dot{\gamma}$. Usually $\eta(\dot{\gamma})$ is a monotonically decreasing function of the shear rate, and the behaviour of the fluid is said to be "shear-thinning". However, in some few cases, the viscosity increases with the shear rate, and the fluid is "shear thickening".
- The first normal stress difference $N_1(\dot{\gamma})$ is positive for polymeric liquids. The first normal stress difference gives rise to the most typical demonstrations of non-Newtonian behaviours, such as the rod-climbing (or Weissenberg) effect, and the very large extrudate swelling at the exit of a die.
- The second normal stress difference $N_2(\dot{\gamma})$ it negative. That quantity is difficult to measure for it is very small. (Approximately an order of magnitude smaller than the first normal stress difference.)

For small values of the shear rate, the first normal stress difference is proportional to $\dot{\gamma}^2$. This is the reason why, in the literature, the normal stress coefficients $\psi_1(\dot{\gamma})$ and $\psi_2(\dot{\gamma})$ are often used instead of $N_1(\dot{\gamma})$ and $N_2(\dot{\gamma})$ to characterize the normal stress differences. The normal stress coefficients are related to the normal stress differences by

$$N_1(\dot{\gamma}) = \psi_1(\dot{\gamma})\dot{\gamma}^2, \qquad N_2(\dot{\gamma}) = \psi_2(\dot{\gamma})\dot{\gamma}^2.$$

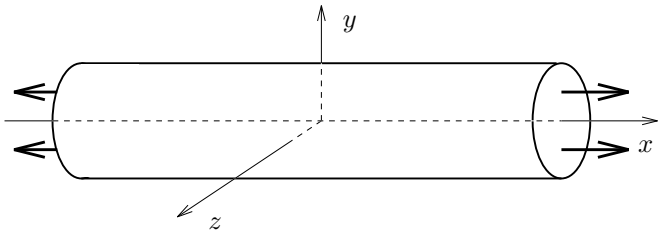

Figure 1.2: *Steady uniaxial extensional flow.*

In steady uniaxial extensional flow (Figure 1.2), the components of the velocity field may be written

$$u = \dot{\epsilon}x, \qquad v = -\frac{\dot{\epsilon}}{2}y, \qquad w = -\frac{\dot{\epsilon}}{2}z,$$

where $\dot{\epsilon}$ is the constant elongational rate. The non-vanishing stresses may be written

$$\sigma_{xx} - \sigma_{yy} = \sigma_{xx} - \sigma_{zz} = \eta_E(\dot{\epsilon})\dot{\epsilon},$$

in which we have introduced $\eta_E(\dot{\epsilon})$ the extensional viscosity.

For Newtonian fluids, Trouton demonstrated that $\eta_E(\dot{\epsilon})$ is a constant equal to thrice the shear viscosity [Tro06]. For non-Newtonian fluids η_E is a function of the extension rate $\dot{\epsilon}$. The qualitative behaviour of the extensional viscosity is often dramatically different from the behaviour of the shear viscosity. For example, the extensional viscosity of highly elastic polymeric fluids usually exhibits a very large increase with the extension rate while the shear viscosity decreases with the shear rate.

Another difference with Newtonian fluids is the "memory" of some non-Newtonian fluids; because of their memory, such fluids behave like elastic materials when submitted to rapid deformations, and more like Newtonian fluids for slow deformations. Such fluids are called "viscoelastic".

A common way to measure the viscoelasticity is by stress relaxation. When a polymeric liquid is submitted to a step increase in strain, the stress also increases in a step, and then decreases exponentially [Mac94]. This behaviour is often represented as a series combination of springs (elastic elements) and dashpots (viscous elements) as represented in Figure 1.3.

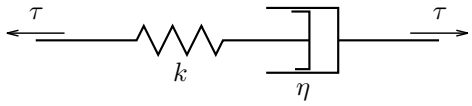

Figure 1.3: *Spring and dashpot representation of a viscoelastic fluid.*

1.2.3 General principles for constitutive equations

The search for constitutive equations describing rheologically complex fluids is the purpose of theoretical rheology. The constitutive equations must satisfy four admissibility conditions:

- The *principle of determinism of stress* states that the stress in a non-Newtonian body is determined by the history of the motion of that body [TN65].
- The *principle of local action* states that the stress at a material point is determined by the history of the deformation of an arbitrarily small neighbourhood around that material point [TN65].
- The *principle of coordinates invariance* states that the constitutive equation must be independent of the frame of reference used to describe them. Expressing the equations in consistent tensorial form will ensure that this principle is automatically satisfied.
- According to the *principle of invariance under superposed rigid body motion*, the rheological equations must have a significance which is independent of absolute motion in space [Old50]. If the equation is correct, any

superimposed rigid body motion cannot affect the basic response of the material.

Although there exists a plethora of constitutive equations in the literature, we will only mention a few ones

Maxwell models

The one-dimensional linear equation of Maxwell is obtained by putting an Hookean spring of constant k and a Newtonian dashpot of viscosity η in series (Figure 1.3). By noting $\dot{\gamma}$ the strain rate of the series, τ will satisfy the differential equation

$$\tau + \lambda\dot{\tau} = \eta\dot{\gamma}, \tag{1.10}$$

with $\lambda = \eta/k$ a relaxation time.

The generalisation of relation (1.10) has to satisfy the principle of objectivity. This leads respectively to the "upper-convected" and "lower-convected" Maxwell models, given respectively by

$$\boldsymbol{T} + \lambda\overset{\triangledown}{\boldsymbol{T}} = 2\eta\boldsymbol{D}, \tag{1.11}$$

and

$$\boldsymbol{T} + \lambda\overset{\triangle}{\boldsymbol{T}} = 2\eta\boldsymbol{D}. \tag{1.12}$$

In equations (1.11) and (1.12), the symbols $\triangledown$ and $\triangle$ stand respectively for the upper-convected and lower-convected derivatives defined by

$$\overset{\triangledown}{\boldsymbol{T}} = \frac{D\boldsymbol{T}}{Dt} - \boldsymbol{L}\cdot\boldsymbol{T} - \boldsymbol{T}\cdot\boldsymbol{L}^{\mathrm{T}}, \tag{1.13}$$

$$\overset{\triangle}{\boldsymbol{T}} = \frac{D\boldsymbol{T}}{Dt} + \boldsymbol{T}\cdot\boldsymbol{L} + \boldsymbol{L}\cdot\boldsymbol{T}^{\mathrm{T}}. \tag{1.14}$$

The upper-convected and lower-convected Maxwell models are also called repsectively "Maxwell-B" and "Maxwell A".

Both Maxwell-A and Maxwell-B have a constant shear viscosity η, and a first normal stress difference quadratic in $\dot{\gamma}$: $N_1(\dot{\gamma}) = 2\eta\lambda\dot{\gamma}^2$. The Maxwell-B model predicts $N_2 = 0$, but for the Maxwell-A model, we have $N_2 = -N_1$. This value of second normal stress difference is much larger than what is experimentally observed. Therefore, the Maxwell-A model is generally not considered. The steady state extensional viscosity of Maxwell-B fluid is

$$\eta_E(\dot{\epsilon}) = \frac{2\eta}{1-2\lambda\dot{\epsilon}} + \frac{\eta}{1+\lambda\dot{\epsilon}}. \tag{1.15}$$

With this formula, an infinite value of the extensional viscosity is obtained for $\dot{\epsilon} = 1/2\lambda$. For higher values of $\dot{\epsilon}$, the expression of the extensional viscosity is meaningless. Indeed, for $\dot{\epsilon} > 1/2\lambda$ it is not possible to reach the steady steady state value (1.15) by a transient calculation starting from vanishing initial stresses because extensional stress grows towards infinity.

Oldroyd-B model

In order to model the behaviour of a polymer solution in a Newtonian solvent, the extra-stress tensor $\boldsymbol{T}$ is often split in two components: a viscoelastic one $\boldsymbol{T}_V$, and a purely viscous one $\boldsymbol{T}_N$. The components $\boldsymbol{T}_V$ and $\boldsymbol{T}_N$ satisfy respectively the relations

$$\boldsymbol{T}_V + \lambda \overset{\triangledown}{\boldsymbol{T}}_V = 2\eta_V \boldsymbol{D},$$
$$\boldsymbol{T}_N = 2\eta_N \boldsymbol{D}.$$

The constitutive equation of the Oldroyd-B model may also be written

$$\boldsymbol{T} + \lambda \overset{\triangledown}{\boldsymbol{T}} = 2\eta \left(\boldsymbol{D} + \lambda_R \overset{\triangledown}{\boldsymbol{D}} \right), \tag{1.16}$$

in which $\eta = \eta_V + \eta_N$ is the constant shear viscosity and $\lambda_R = \eta_N \lambda / \eta$ is a retardation time. The normal stress differences of the Oldroyd-B model are $N_1(\dot{\gamma}) = 2\eta_V \lambda \dot{\gamma}^2$ and $N_2 = 0$. The steady extensional viscosity is given by

$$\eta_E(\dot{\epsilon}) = \frac{2\eta_V}{1 - 2\lambda\dot{\epsilon}} + \frac{\eta_V}{1 + \lambda\dot{\epsilon}} + 3\eta_N.$$

Johnson-Segalman model

The second normal stress difference may be related to the presence of a lower convected derivative in the constitutive equations. The Johnson-Segalman model is defined by the constitutive equation

$$\boldsymbol{T} + \lambda \overset{\square}{\boldsymbol{T}} = 2\eta_0 \boldsymbol{D}, \tag{1.17}$$

in which $\overset{\square}{\boldsymbol{T}}$ is a convex combination of the upper and lower convected derivatives:

$$\overset{\square}{\boldsymbol{T}} = \left(1 - \frac{\xi}{2}\right) \overset{\triangledown}{\boldsymbol{T}} + \frac{\xi}{2} \overset{\triangle}{\boldsymbol{T}},$$

ξ being a scalar parameter ($0 \leq \xi \leq 2$).

The Johnson-Segalman model predicts shear-thinning viscosity, first and second normal stress differences:

$$\eta(\dot{\gamma}) = \frac{\eta_0}{1 + \xi(2 - \xi)\lambda^2\dot{\gamma}^2},$$
$$\psi_1(\dot{\gamma}) = \frac{2\lambda\eta_0}{1 + \xi(2 - \xi)\lambda^2\dot{\gamma}^2},$$
$$\psi_2(\dot{\gamma}) = \frac{-\xi\lambda\eta_0}{1 + \xi(2 - \xi)\lambda^2\dot{\gamma}^2}.$$

For this model, $N_2/N_1 = -\xi/2$. The value $\xi = 0.2$, gives a ratio $N_2/N_1 = -0.1$ corresponding to what is experimentally observed. The steady extensional viscosity exhibited by the Johnson-Segalman model is equal to that of the Maxwell-B model. The shear viscosity tends towards zero when the shear rate tends towards infinity. This problem may be avoided by adding a purely viscous component to the extra-stress tensor.

Phan-Thien-Tanner model

The extensional viscosity of the Johnson-Segalman model tends towards infinity when the extension rate tends towards $1/2\lambda$. The constitutive equation (1.17) may be modified to avoid that problem:

$$\exp\left(\frac{\epsilon_{\mathrm{PTT}}\lambda}{\eta_0}\right)\boldsymbol{T} + \lambda\overset{\square}{\boldsymbol{T}} = 2\eta_0\boldsymbol{D}. \tag{1.18}$$

Here again, a purely viscous component may be added to the extra-stress tensor. In general, no analytical expression may be found for the viscosities and normal stress differences with the PTT model.

Giesekus model

The constitutive equation defining the Giesekus model is given by

$$\boldsymbol{T} + \lambda\overset{\triangledown}{\boldsymbol{T}} + \frac{\alpha_{\mathrm{G}}\lambda}{\eta_V}\boldsymbol{T}\cdot\boldsymbol{T} = 2\eta_V\boldsymbol{D}. \tag{1.19}$$

This model exhibits both first and second normal stress differences. With this model, one obtains excellent fits in shear flows, but the extensional behaviour is not very good.

Criminale-Ericksen-Filbey model

The Criminale-Ericksen-Filbey model is a generalisation of the second-order fluid [BHAC77, Lar88]:

$$\boldsymbol{T} = 2\eta_0\boldsymbol{D} - \psi_{10}\overset{\triangledown}{\boldsymbol{D}} + 4\psi_{20}\boldsymbol{D}\cdot\boldsymbol{D}. \tag{1.20}$$

The generalisation is obtained by replacing the constants η_0, $\psi_{1,0}$ and $\psi_{2,0}$ by functions of the shear rate $\dot{\gamma}$:

$$\boldsymbol{T} = 2\eta(\dot{\gamma})\boldsymbol{D} - \psi_1(\dot{\gamma})\overset{\triangledown}{\boldsymbol{D}} + 4\psi_2(\dot{\gamma})\boldsymbol{D}\cdot\boldsymbol{D}. \tag{1.21}$$

The Criminale-Ericksen-Filbey model is not a viscoelastic model, for the model exhibits no memory effect: the extra-stress tensor $\boldsymbol{T}$ at a given time only depends on the velocity field at the same time. The model cannot be expected to predict time-dependent phenomena.

Reiner-Rivlin model

The Criminale-Ericksen-Filbey model may be simplified by neglecting ψ_1 in (1.21). This leads to the Reiner-Rivlin model:

$$\boldsymbol{T} = 2\eta(\dot{\gamma})\boldsymbol{D}(\boldsymbol{v}) + 4\psi_2(\dot{\gamma})\boldsymbol{D}(\boldsymbol{v})\cdot\boldsymbol{D}(\boldsymbol{v}). \tag{1.22}$$

This model may be easier to use for numerical calculations: equation (1.22) only involves first order spatial derivatives of the velocity field. This allows us to substitute $\boldsymbol{T}$ in the momentum equations with the right member of (1.22). With such a substitution, the weak form of the momentum equation only involves first order spatial derivatives of the velocity field.

As a comparison, the extra-stress tensor of the Criminale-Ericksen-Filbey model, though exhibiting no memory effects, involves second order spatial derivatives of $\boldsymbol{v}$ because of the upper-convected derivative of $\boldsymbol{D}$. Therefore, to calculate a complex flow with the finite element method with such a model, an extra field $\boldsymbol{D}$ must be added to the variables of the model.

1.2.4 Derivation of models from a molecular theory

Several reasons justify the molecular approach. First, the rheological properties of polymer solutions and polymer melts depend on the molecular architecture of the constituent molecules (molecular weight, molecular weight distribution, chain stiffness). Second, solute-solvent interactions can play a role in the motion of the polymers and affect their macroscopic behaviour. Third, in the neighbourhood of fluid-solid interface, the motion of the polymer molecules is restricted, with the result that wall slip can arise. Finally, useful relationships can be derived between the rheological properties and other physico-chemical properties, such as the diffusional, optical and electrical properties.

The theories deal either with dilute solutions or with concentrated solutions and molten polymers. In dilute solutions theories, each particle interacts only with the solvent and not with the other suspended particles, while in the concentrated fluid theories there are particle-particle interactions, which may form molecular entanglements.

This section is mainly inspired from Bird et al. [BHAC77], and from the thesis of Bruno Purnode [Pur96]. We first present the Rouse chain and dumbbells molecular models. Then we introduce the kinetic theory for elastic dumbbells. In particular, we develop the macroscopic model corresponding to Hookean dumbbells, and to finitely extensible dumbbells. We will not discuss the network and reptation theories for concentrated solutions and polymer melts.

Let us remark that all constitutive models may be derived from molecular theories. Thus the models presented in section 1.2.3 may also be justified by molecular arguments, and actually, some of them have been derived from a molecular theory. The only purpose of this section is to show how a macroscopic constitutive equation may be derived from a kinetic theory.

Molecular models

Following the theory of Rouse [Rou53], polymer coil can be thought of as a series of spherical beads equally spaced and connected one to the next by springs. Each spring models the elastic forces generated by a portion of the polymer macromolecule called a submolecule (Figure 1.4). The polymer solution is sufficiently dilute to allow us to make the assumption that each molecule is isolated

from the others.

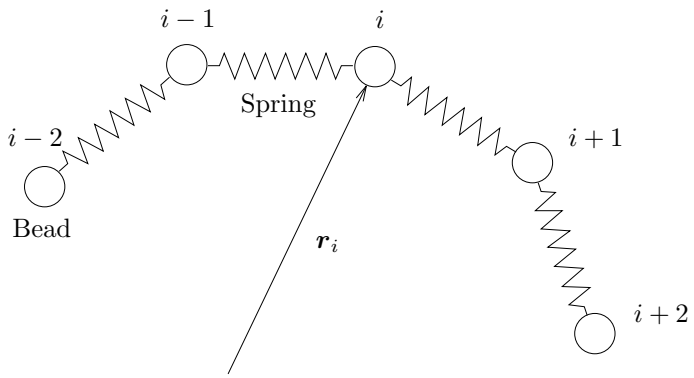

Figure 1.4: *The Rouse bead and spring model for a polymer macromolecule.*

We will here only treat the case of two beads joined by a non-bendable spring: the elastic dumbbell (Figure 1.5). The reason is that the dumbbell theory qualitatively reproduces most features of the Rouse theory. The beads of masses m are labeled with "1" and "2". Their instantaneous location in space are called $\boldsymbol{r}_1$ and $\boldsymbol{r}_2$. The configuration vector $\boldsymbol{R} = \boldsymbol{r}_2 - \boldsymbol{r}_1$ specifies the instantaneous distance between the beads centers and the angular orientation of the dumbbells in space. There are n dumbbells per unit volume suspended in a Newtonian solvent of viscosity η_N.

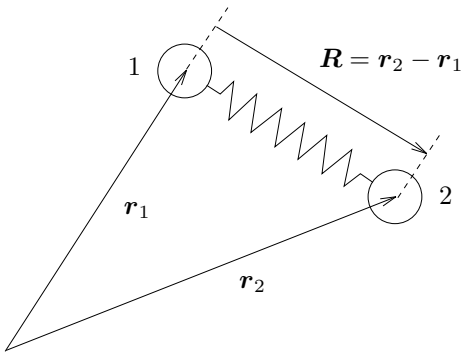

Figure 1.5: *Elastic dumbbell composed of two beads connected by an elastic spring.*

Kinetic theory for dumbbells

The purpose of this section is to show how macroscopic consitutive equations may be derived from a molecular theory. Thus, we do not present the theory and results of stochastic calculations.

In order to derive a macrosocopic model, a distribution function $\psi(\boldsymbol{R}, t)$ is defined. This function gives the probability to find a dumbbell at a given configuration $\boldsymbol{R}$ and for a given time t. The conservation equation for the dumbbells may be written as a function of the distribution function ψ:

$$\frac{\partial \psi}{\partial t} + \frac{\partial}{\partial \boldsymbol{R}} \cdot (\psi \dot{\boldsymbol{R}}) = 0.$$

Taking into account the hydrodynamic drag forces $\boldsymbol{F}^h$, the brownian forces $\boldsymbol{F}^b$ and the connector force $\boldsymbol{F}^c$ in the spring, an equation of change may be written for the average $< \boldsymbol{RR} >$:

$$< \overset{\triangledown}{\boldsymbol{RR}} > + \frac{4}{\zeta} < \boldsymbol{RF}^c >= \frac{4kT}{\zeta} \boldsymbol{I},$$

in which we have introduced the notation

$$< B >= \int B(\boldsymbol{R}) \psi(\boldsymbol{R}, t) d\boldsymbol{R},$$

$B(\boldsymbol{R})$ being a dynamical property depending on $\boldsymbol{R}$, k the Boltzmann constant, n the number of dumbbells per unit of volume and T the temperature. ζ is a friction factor relating the hydrodynamic drag force on a bead to the relative velocity of the bead and the solvent:

$$\boldsymbol{F}^h = \zeta(\boldsymbol{v} - \dot{\boldsymbol{r}}).$$

The dumbbells contribute to the momentum equation by the force of their connector spring, and by the amount of momentum they carry with them. This results in a contribution to the extra-stress tensor given by

$$\boldsymbol{T}_V = n < \boldsymbol{RF}^c > -nkT\boldsymbol{I}. \tag{1.23}$$

The last expression is usually called the Kramers expression for the extra-stress tensor [Kra44].

We will introduce the notations R for the end-to-end distance of the vector $\boldsymbol{R}$, and F such that

$$\boldsymbol{F}^c = F(R)\boldsymbol{R}.$$

With these new notations, the evolution equation for the dumbbells and the expression of the extra-stress tensor are given by

$$< \overset{\triangledown}{\boldsymbol{RR}} > + \frac{4}{\zeta} < F(R)\boldsymbol{RR} >= \frac{4kT}{\zeta} \boldsymbol{I}, \tag{1.24}$$

$$\boldsymbol{T}_V = n < F(R)\boldsymbol{RR} > -nkT\boldsymbol{I}. \tag{1.25}$$

Up to this point, the theory has been developed for dumbbells with any kind of elastic connector. Now we will characterize the connector force law. Although a great number of spring types can be used, we will only consider the Hookean and the Warner force laws.

Hookean dumbbells

Let us first assume that the spring is Hookean, i.e. that the tension in the spring is directly proportional to the separation of the beads:

$$F(R) = H.$$

Then, the Kramers expression for the stress tensor (1.23) gives:

$$\boldsymbol{T}_V = nH < \boldsymbol{RR} > -nkT\boldsymbol{I},$$

whereas the evolution equation for $< \boldsymbol{RR} >$ is given by:

$$< \overset{\triangledown}{\boldsymbol{RR}} > + \frac{4H}{\zeta} < \boldsymbol{RR} >= \frac{4kT}{\zeta}\boldsymbol{I}.$$

Eliminating $< \boldsymbol{RR} >$ from those equations leads to the following rheological equation of state:

$$\boldsymbol{T}_V + \frac{\zeta}{4H}\overset{\triangledown}{\boldsymbol{T}}_V = \frac{n\zeta kT}{2H}\boldsymbol{D},$$

As one defines the characteristic time constant $\lambda = \zeta/4H$ and $\eta_V = n\zeta kT/4H$, this model is the well-known Maxwell-B fluid. By adding a purely viscous component to the constitutive equation, one obtains the Oldroyd-B model.

Fene dumbbells

Let us now consider the Warner force law that avoids the unphysical feature of infinitely extending dumbbells:

$$F(R) = \frac{H}{1 - R^2/R_0^2}.$$

A spring with this force law will be linear for small extensions, but will get ever stiffer as the spring is extended. Furthermore, the spring cannot be extended beyond a separation R_0. This dumbbell with limited extension is also called *Finitely Extensible Nonlinear Elastic* (FENE) dumbbell. Replacing the Warner force law in the evolution equation and the Kramers expression gives:

$$< \overset{\triangledown}{\boldsymbol{RR}} > + \frac{4H}{\zeta} < \frac{1}{1 - R^2/R_0^2}\boldsymbol{RR} >= \frac{4kT}{\zeta}\boldsymbol{I}, \tag{1.26}$$

$$\boldsymbol{T}_V = nH < \frac{1}{1 - R^2/R_0^2}\boldsymbol{RR} > -nkT\boldsymbol{I}. \tag{1.27}$$

It is not possible to eliminate the average values, as it was done for the case of Hookean dumbbells. However, replacing the average of the ratio by the ratio of the averages as suggested by Peterlin [Pet66]:

$$< \frac{H}{1 - R^2/R_0^2}\boldsymbol{RR} >= \frac{H}{1 - < R^2/R_0^2 >} < \boldsymbol{RR} >,$$

leads to a tractable rheological equation of state. Indeed, defining a non-dimensional configuration tensor $\boldsymbol{A}$ and a characteristic dumbbell length R_e as follows:

$$\boldsymbol{A} = \frac{3 < \boldsymbol{RR} >}{R_e^2},$$

$$R_e^2 = \frac{3kT}{F(R_e)},$$

and replacing in the equations 1.26 and 1.27 we obtain the following governing equations for fields $\boldsymbol{A}$ and $\boldsymbol{T}_V$:

$$\boldsymbol{A} + \lambda(1 - \mathrm{tr}\boldsymbol{A}/L^2)\overset{\triangledown}{\boldsymbol{A}} = \frac{1 - \mathrm{tr}\boldsymbol{A}/L^2}{1 - 3/L^2}\boldsymbol{I}, \tag{1.28}$$

$$\boldsymbol{T}_V = \frac{\eta_V}{\lambda}\left(\frac{1}{1 - \mathrm{tr}\boldsymbol{A}/L^2}\boldsymbol{A} - \frac{1}{1 - 3/L^2}\boldsymbol{I}\right), \tag{1.29}$$

where $L^2 = 3R_0^2/R_e^2$ is a measure of the extensibility of the dumbbells, λ is the relaxation time, and η_V is the viscoelastic part of viscosity. The relaxation time and the zero-shear viscosity are defined by:

$$\lambda = \frac{\zeta}{4H}, \quad \eta_V = \frac{n\zeta kT}{4H}(1 - 3/L^2).$$

This fluid is called the FENE-P model [BDJ80]. This formulation, based on the configuration tensor, is known to offer stable numerical properties [AH94]. The fluid exhibits shear thinning behaviour, and for high shear rates, η is proportional to $\dot{\gamma}^{-2/3}$. At high shear rates, the first normal stress difference scales as $\dot{\gamma}^{2/3}$. The second normal stress N_2 is vanishing. In extensional flow, the model also exhibits an extensional thickening behaviour, and reaches a plateau at high extension rates.

Chilcott and Rallison [CR88] proposed some further modifications in the evolution for $\boldsymbol{A}$ in order to obtain a fluid with a constant viscosity in steady shear flow:

$$\boldsymbol{A} + \lambda(1 - \mathrm{tr}\boldsymbol{A}/L^2)\overset{\triangledown}{\boldsymbol{A}} = \boldsymbol{I}. \tag{1.30}$$

The equation giving the extra-stress tensor is identical to (1.29). Equations (1.29) and (1.30) define the FENE Chilcott-Rallison model (FENE-CR). This model shows a first normal stress difference that changes from quadratic to linear behaviour as shear rate increases.

1.2.5 Dimensionless numbers for viscoelastic flows

Dimensionless numbers are generally used to characterize fluid mechanics problems. For example, the Reynolds number defined by

$$I\!R = \frac{\rho V L}{\eta}$$

in which V and L are characteristic velocity and length of the problem respectively. $I\!R$ characterizes the importance of inertia forces with respect to viscous forces. It may be used to characterize both Newtonian and non-Newtonian flows.

The viscoelasticity of a flow may be characterized by the Weissenberg number, We. It is defined as

$$\mathrm{We} = \frac{\lambda V}{L},$$

in which λ is a characteristic relaxation time. It may be interpreted as a ratio of normal stresses and shear stress.

For transient flow, The Deborah number De is often used. It is defined as the ratio of a characteristic time λ of the fluid and a characteristic time of the flow t_c:

$$\mathrm{De} = \frac{\lambda}{t_c}.$$

1.3 Spatial discretization for viscoelastic flows

1.3.1 Galerkin method

In this section, we wish to describe the numerical problem of the simulation of viscoelastic fluids. For convenience, we will limit ourselves to the steady flow of a Maxwell fluid in a differential form, and to the finite element formulation. The strong formulation of the system of partial differential equations is then given by

$$\begin{aligned} \boldsymbol{T} + \lambda \overset{\triangledown}{\boldsymbol{T}} &= 2\eta_V \boldsymbol{D}(\boldsymbol{v}), \\ -\nabla \cdot p + \nabla \cdot \boldsymbol{T} + \boldsymbol{f} &= \boldsymbol{0}, \\ \nabla \cdot \boldsymbol{v} &= 0. \end{aligned}$$

We assume that the flow domain is discretized by means of a mesh of finite elements and we approximate the viscoelastic stresses, the velocity and the pressure by means of the finite expansions

$$\begin{aligned} \boldsymbol{T}^h &= \sum_{i=1}^{N_T} \boldsymbol{T}_i \phi_i, \\ \boldsymbol{v}^h &= \sum_{j=1}^{N_v} \boldsymbol{v}_j \psi_j, \\ p^h &= \sum_{k=1}^{N_p} p_k \pi_k, \end{aligned}$$

in which ϕ_i, ψ_j and π_k are the shape functions and $\boldsymbol{T}_i$, $\boldsymbol{v}_j$ and p_k are the unknown nodal values.

In order to calculate the nodal variables, the classical Galerkin procedure imposes that the governing equations are orthogonal to the set of shape functions. Finally, an integration by parts in the momentum equations is used to yield the discrete problem:

$$\begin{aligned}
\int_\Omega \phi_i \left(\boldsymbol{T}^h + \lambda \overset{\triangledown}{\boldsymbol{T}^h} - 2\eta_V \boldsymbol{D}(\boldsymbol{v}^h) \right) \mathrm{d}\Omega &= 0 && i = 1 \cdots N_T, \\
\int_\Omega \left(\boldsymbol{\nabla}\psi_j \cdot \left(-p^h \boldsymbol{\delta} + \boldsymbol{T}^h \right) - \psi_j \boldsymbol{f} \right) \mathrm{d}\Omega &= \int_{\partial\Omega} \psi_j \boldsymbol{\sigma} \cdot \boldsymbol{n} \mathrm{d}s && j = 1 \cdots N_v, \\
\int_\Omega \pi_k \left(\nabla \cdot \boldsymbol{v}^h \right) \mathrm{d}\Omega &= 0 && k = 1 \cdots N_p,
\end{aligned} \tag{1.31}$$

where Ω is the domain on which the calculations are done, $\partial\Omega$ is the boundary of the domain, $\boldsymbol{n}$ is the outward unit normal vector, and s is the curvilinear coordinate along the boundary. This procedure reduces the continuity requirements imposed for the discrete velocity field and it allows the specification of natural boundary conditions in terms of the contact force $\boldsymbol{t} = \boldsymbol{\sigma} \cdot \boldsymbol{n}$ along the boundary. Essential (or Dirichlet) boundary conditions also may be imposed on the momentum equations (i.e. on the velocities). (More details on the imposition of Dirichlet boundary conditions are given in section C.1). The set of equations (1.31) defines formulation MIX-1 [KT77, CK80].

1.3.2 Interpolations

The precision of the solution obtained by the finite element method depends on the choice of interpolant for the unknown fields. The observation of the discretized equations (1.31) shows that the shape functions for the extra-stresses and velocities must be continuous, but the shape functions for pressure only have to be piece-wise continuous.

If we consider a classical mixed velocity-pressure formulation, the mixed interpolation must satisfy a compatibility condition derived by Ladyzhenskaya, Babuska and Brezzi [Bre74] in order to provide stable results. The popular choice of quadratic velocity interpolation with a linear pressure may be justified by the so-called LBB condition.

For the MIX-1 formulation, the first most widely used mixed interpolation, in the case of quadrilateral elements was the following:

- The viscoelastic extra-stress was approximated by means of biquadratic polynomials.
- The basis function for the pressure and the velocity fields are respectively bilinear and biquadratic polynomials. This choice was directly inspired by the LBB condition for the velocity-pressure formulation.

For this choice, all fields were continuous over the flow domain.

In the Newtonian limit $\lambda \to 0$, and for a quadratic interpolation for the extra-stresses, equations (1.31) are not equivalent to the classical Galerkin for-

mulation of the Navier-Stokes equations. Moreover, Newtonian results of MIX-1 are oscillatory in flows with high gradients.

This fact has been used by Marchal and Crochet [MC86] in the special case of rectangular elements. They found that a sufficient condition for the mixed method to reproduce results identical to those of the velocity-pressure formulation in the Newtonian case was that the discrete stress space must contain the gradient of the discrete velocity space [MC87]. In particular, they modified the stress interpolation as follows: the basic nine-nodes element for the velocity is subdivided into 4×4 bilinear subelements for the stresses (Figure 1.6). Such a mixed finite element was found to give excellent results for the Newtonian case, even near stress boundary layers. This particular element defines the so-called 4×4 formulation which does not however break the high Weissenberg number problem (i.e.the calculation of a flow with the finite element methods become generally difficult when We is increased).

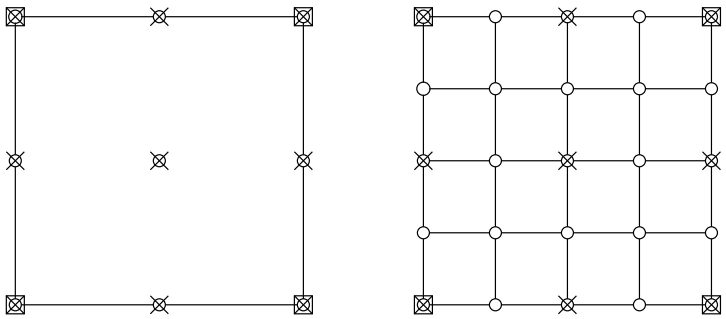

Figure 1.6: *Description of mixed interpolants for the finite element simulation of viscoelastic flows: MIX-1 formulation (a) and* 4×4 *element (b). The circles represent the extra-stress nodes, the crosses the velocities and the squares the pressure.*

The main drawback of this method is its large computational cost. Other methods like the EVSS formulation have been proposed to calculate viscoelastic flows (section 1.3.3).

1.3.3 Stress-splitting formulations

In the limit of Newtonian flows ($\lambda = 0$), the MIX formulation in terms of $(\boldsymbol{T}, \boldsymbol{v}, p)$ is not equivalent to the usual $(\boldsymbol{v}, p)$ formulation of the Stokes equations. When we introduce the discretization, this fact has detrimental numerical implications [Keu89] and can be circumvented with the following change of variables:

$$\boldsymbol{S} = \boldsymbol{T} - 2\eta \boldsymbol{\mathcal{D}}(\boldsymbol{v}).$$

A convected derivative of $\boldsymbol{\mathcal{D}}(\boldsymbol{v})$ is then introduced in the constitutive equation, involving second-order spatial derivatives of $\boldsymbol{v}$. But, these derivatives can be

eliminated by considering a $(\boldsymbol{S}, \boldsymbol{v}, p, \boldsymbol{D})$ approximation. In order to define the *Elastic Viscous Split Stress formulation* (EVSS), Rajagopalan et al. [RBA90] introduced the modified stress tensor $\boldsymbol{S}$ and the rate of deformation $\boldsymbol{D}$ as additional unknowns, in the following way:

$$\begin{aligned} \boldsymbol{S} &= \boldsymbol{T} - 2\eta\boldsymbol{D}, \\ \boldsymbol{D} &= \frac{1}{2}(\nabla\boldsymbol{v} + \nabla\boldsymbol{v}^{\mathrm{T}}). \end{aligned} \tag{1.32}$$

The discretization of the EVSS formulation provides more stable and accurate solutions than the discretization of the MIX formulation. Those good numerical properties are due both to a new elliptic stabilizing term in the momentum equation and to the least-square approximation of $\boldsymbol{\mathcal{D}}(\boldsymbol{v})$ by a new variable $\boldsymbol{D}$.

In order to further improve the numerical properties, Sun et al. [SPTT96] proposed a modified version of the EVSS formulation to compute the flow of the upper-convected Maxwell fluid. Their so-called reference viscosity scheme formulation can be written as follows:

$$\boldsymbol{S} = \boldsymbol{T} - 2\beta\boldsymbol{D}, \tag{1.33}$$

where the reference viscosity β is a function of the coordinates and can be much larger than η used in the usual EVSS formulation. In other words, the EVSS formulation is a particular case of this formulation. They also proposed an adaptive procedure to select β so as to obtain a viscous stress $2\beta\boldsymbol{\mathcal{D}}(\boldsymbol{v})$ at least of the same order as the elastic stress $\boldsymbol{S}$. This scheme defines the so-called *Adaptive Viscous Stress Splitting formulation* (AVSS).

In order to introduce a similar elliptic stabilizing term in the momentum equations for other models, Guénette and Fortin [GF95] considered a modified stress splitting formulation. No change of variable is applied but the momentum equations are modified as follows:

$$\nabla \cdot \sigma(\boldsymbol{T}, p) + 2\alpha\nabla \cdot (\boldsymbol{\mathcal{D}}(\boldsymbol{v}) - \boldsymbol{D}) = \boldsymbol{0}.$$

Obviously, $\boldsymbol{\mathcal{D}}(\boldsymbol{v}) - \boldsymbol{D}$ vanishes in the continuous formulation, but it is introduced here as a stabilization term in the momentum equations. It acts exactly as the additional term generated by the change of variable of the EVSS formulation. This is sometimes known as the *Discrete Elastic Viscous Stress Splitting formulation* (DEVSS) or as the extended EVSS formulation of Guénettte and Fortin.

All those formulations are particular cases of the following generic problem:

Find $(\boldsymbol{S},\ \boldsymbol{v},\ p,\ \boldsymbol{D})$ *such that*

$$\begin{aligned} \boldsymbol{S} + \lambda(\overset{\triangledown}{\boldsymbol{S}} + 2\beta\overset{\triangledown}{\boldsymbol{D}}) - 2(\eta - \beta)\boldsymbol{\mathcal{D}}(\boldsymbol{v}) &= \boldsymbol{0}, \\ \nabla \cdot (-p\boldsymbol{I} + \boldsymbol{S} + 2\beta\boldsymbol{\mathcal{D}}(\boldsymbol{v})) + 2\alpha\nabla \cdot (\boldsymbol{\mathcal{D}}(\boldsymbol{v}) - \boldsymbol{D}) &= \boldsymbol{0}, \\ \nabla \cdot \boldsymbol{v} &= \boldsymbol{0}, \\ \boldsymbol{D} - \boldsymbol{\mathcal{D}}(\boldsymbol{v}) &= \boldsymbol{0}. \end{aligned}$$

Note that we only present the generic problem on the example of the Maxwell model. But the generic formulation may easily be generalized to more complicated constitutive equations.

The MIX formulation corresponds to the case $\alpha = \beta = 0$ (the field $\boldsymbol{D}$ is then not required and the field $\boldsymbol{S}$ becomes $\boldsymbol{T}$) and the standard EVSS method (1.32) can be obtained with $\alpha = 0$, $\beta = \eta$. We obtain the reference viscosity AVSS formulation (1.33) with $\alpha = 0$ and the extended EVSS formulation of Guénette et al. with $\beta = 0$.

1.3.4 Interpolations for 3D calculations

There is no general mathematical theory that would give the choice of the approximations of the extra-stress tensor to be used with the various viscoelastic formulations. In this thesis, we only use the DEVSS formulation for the 3D coextrusion calculations (chapter 3).

An interesting property of the extended EVSS formulation is that, after integration by parts of the momentum equation, the tensor $\boldsymbol{D}$ appears under an algebraic form in the formulation. This allows us to use a discontinuous interpolation for that field, and may lead to dramatic reduction of computational cost, especially for 3D calculations.

Thus, for those calculations, we use a trilinear interpolation for the extra-stress tensor. For the velocities and pressure, we use the mini-element of Fortin [For81] (pressure is discontinuous and constant on the elements, velocities are trilinear, but one adds a normal degree of freedom at the center of each face). For the tensor $\boldsymbol{D}$ we use the same type of interpolation as for the pressure.

Note that for the 3D Newtonian and Reiner-Rivlin calculations, the mini-element of Fortin is also used for the velocity and pressure discretization.

1.3.5 Upwinding

It is possible to demonstrate that the classical Galerkin formulation is optimal for the discretization of elliptic equations. But the equations governing viscoelastic flows are hyperbolic. The streamline upwind Petrov-Galerkin (SUPG) method has been developed by Brooks et al. [BH82] in order to provide stable and accurate formulation for advection-diffusion equations. This technique consists in replacing the weight function ψ_i of the constitutive equation by

$$\hat{\psi}_i = \psi_i + k\boldsymbol{v} \cdot \nabla\psi_i,$$

where k is a scalar of the order of the finite element size h.

Numerical experiments and mathematical analysis establish that, for a given velocity field, the SUPG is more accurate and stable. However, when Marchal and Crochet have incorporated the 4×4 interpolation and the SUPG technique for the problem of the full set of viscoelastic equations, they have obtained oscillatory extra-stress and velocity at relatively small values of the Weissenberg number, even if interesting accurate results can be obtained for the flow around a sphere or in undulated channels.

Therefore, Marchal and Crochet used the SU method. In this approach, the additional term of the test function affects only the purely advective term $\boldsymbol{v}^h \cdot \nabla \boldsymbol{T}^h$ of the upper convective derivative. The SU method has very good stability properties, but is only first-order accurate. In other words, the artificial diffusion of the SU algorithm introduces an error proportional to the size of elements. But with SU, solutions have been obtained at very high Weissenberg numbers using Maxwell and Oldroyd-B fluids in flows with and without stress singularities [CAD+95a].

1.3.6 Stream function

For two-dimensional calculations, if the divergence of velocity field vanishes (incompressible flow), the components of the velocity may be derived from a scalar stream function ψ. For example, for a planar flow, we have

$$u = \psi_{,y} \text{ and } v = -\psi_{,x},$$

in which $\{x, y\}^{\mathrm{T}}$ are the coordinate components, and $\{u, v\}^{\mathrm{T}}$ the velocity components.

This function is often used to visualize flows, for isolines of the stream function given by the solution of

$$\psi(x, y) = \text{constant}$$

are parallel to the direction of velocity vectors.

It easily can be shown that ψ is the solution of a Poisson equation. Indeed, by defining the vector

$$\left\{ \begin{array}{c} \psi_{,x} \\ \psi_{,y} \end{array} \right\} = \left\{ \begin{array}{c} -v \\ u \end{array} \right\},$$

and calculating its divergence, one obtains

$$\nabla^2 \psi = -v_{,x} + u_{,y}. \tag{1.34}$$

A similar transformation may be done for axisymmetric flows.

An interesting characteristic of equation (1.34) is that ψ is the solution of an elliptic Poisson equation. This ensures that isolines are generally smooth, even when the velocity field presents wiggles.

1.3.7 Solution of the nonlinear system

The discretization of the governing equations with the finite element method leads to a system of nonlinear equations. Two basic approaches have been adopted to solve the nonlinear system:

- In the *coupled* approach, the equations are solved simultaneously for the whole set of variables. The advantage of this approach lays in the possibility of deriving Newton-Raphson's or Picard's equations for solving the nonlinear problem (section A.2). Its disadvantage is the relatively high computer cost caused by fairly large number of variables.

- In the *decoupled* approach, the calculation of the viscoelastic extra-stress is performed separately from the flow kinematics: from known velocity and pressure, one calculates the extra-stress by integrating the constitutive equations; then, the kinematics is updated by solving the conservation equations for a given extra-stress. With this approach, the number of variables is much lower than in the coupled approach, but the number of iterations is also much larger because it does not enjoy the quadratic convergence properties of Newton's method (section A.2).

1.4 Time discretization

In this section, we present the methods used to discretize the equations in time. This discretization in time has to be done if a time derivative appears in the governing equations. A general form of the time dependent equations is

$$\mathbf{M}(\mathbf{z})\dot{\mathbf{z}} + \mathbf{g}(\mathbf{z}) = \mathbf{0}, \tag{1.35}$$

where $\mathbf{z}$ is the vector containing the nodal values, $\mathbf{M}$ is the mass matrix, and $\mathbf{g}(\mathbf{z})$ is a vector. An initial condition is given to the solution at time t_0:

$$\mathbf{z}(t_0) = \mathbf{z}_0.$$

The time discretization of equation (1.35) consists in finding numerical approximations $\mathbf{z}^n$ of the unknown theoretical solution $\mathbf{z}(t)$ at discrete times t_n defined by $t_0 < t_1 < \cdots < t_n < \cdots < t_N$.

In this thesis, we only use algorithms derived from the θ methods. Equation (1.35) also may be written

$$\dot{\mathbf{z}} = -\mathbf{M}^{-1}(\mathbf{z})\mathbf{g}(\mathbf{z}). \tag{1.36}$$

The discretization of this equation with a θ scheme gives

$$\frac{\mathbf{z}^{n+1} - \mathbf{z}^n}{\Delta t_{n+1}} = -\theta\mathbf{M}^{-1}(\mathbf{z}^{n+1})\mathbf{g}(\mathbf{z}^{n+1}) - (1-\theta)\mathbf{M}^{-1}(\mathbf{z}^n)\mathbf{g}(\mathbf{z}^n), \tag{1.37}$$

in which $\Delta t_{n+1} = t_{n+1} - t_n$ is the time step and θ controls the implicit character of the time discretization.

The values $\theta = 0$ and $\theta = 1$ give the explicit and implicit Euler schemes respectively. Both Euler schemes are first order schemes. The value $\theta = 1/2$ gives the second order Crank-Nicolson method. The value $\theta = 2/3$ gives a first order scheme called "Galerkin method". More informations about the implementation of the θ methods are given in section A.3.

It is important to know whether a transient method is stable or not. For advection equations, it has been shown that among the θ methods, the criterion of stability is $\theta \geq \frac{1}{2}$. This means that Cranck-Nicolson, Galerkin and implicit Euler schemes are unconditionnally stable; but explicit Euler scheme is unconditionnally unstable. This is related to the fact that the time discretization

of an advection equation with the explicit Euler schemes introduces an artificial negative diffusion. with Galerkin and implicit Euler schemes, the artificial diffusion is positive. Numerical diffusion vanishes for $\theta = \frac{1}{2}$. Consequently, the Cranck-Nicolson scheme is adpated to the study of stability by transient integration.

1.5 Free surfaces

In this thesis, we calculate flows on geometries with free surfaces or interfaces. Kinematic conditions are used to calculate the motion of those moving boundaries. In order to avoid overdistorded elements inside the computational domain, the motion of the boundaries must be propagated inside the mesh. This is done with an appropriate remeshing technique.

1.5.1 Kinematic conditions

The kinematic condition expresses the condition that fluids do not flow across free surfaces or interfaces. The simplest way to express such a condition is the following:

$$(\boldsymbol{v} - \dot{\boldsymbol{x}}) \cdot \boldsymbol{n} = 0, \tag{1.38}$$

in which $\boldsymbol{v}$ is the fluid velocity, $\dot{\boldsymbol{x}}$ is the time derivative of eulerian coordinates and $\boldsymbol{n}$ is the normal vector to the moving surface. Thus, $\boldsymbol{n}$ depends on the coordinates on this surface. The difference $\boldsymbol{v} - \dot{\boldsymbol{x}}$ is the fluid velocity relative to the mesh. By mutliplying this relative velocity by the normal to the boundary we obtain the flow rate through this surface. Thus, we impose this surface flow rate to vanish at each point along this surface. Equation (1.38) may be discretized using a Galerkin formulation for two- and three-dimensional flows. It will be referred to as "surface kinematic condition" in the next chapters. For time independent flows, $\dot{\boldsymbol{x}} = \boldsymbol{0}$ and (1.38) reduces to $\boldsymbol{v} \cdot \boldsymbol{n} = 0$.

To calculate the motion of a free surface, another type of kinematic condition called "line kinematic condition" may be used; the mesh of the moving surface is divided in lines. Each line is constrained to be parallel to the velocity (Figure 1.7). It is possible to show that this method is optimal because the kinematic condition leads to hyperbolic equations. The use of this method requires the structure of the mesh to be such that it can easily be divided in lines parallel to the main direction of flow. Thus, it also requires a good knowledge of the main direction of flow prior to its calculation. Those two characteristics of the line kinematic condition restrict its use to the calculation of free surface extrusion flows.

Let us define a unit vector $\boldsymbol{\tau}$ tangent to a mesh line with

$$\boldsymbol{\tau} = \frac{\boldsymbol{x}_s}{||\boldsymbol{x}_s||},$$

in which s is a curvilinear coordinate following the mesh line. The equation

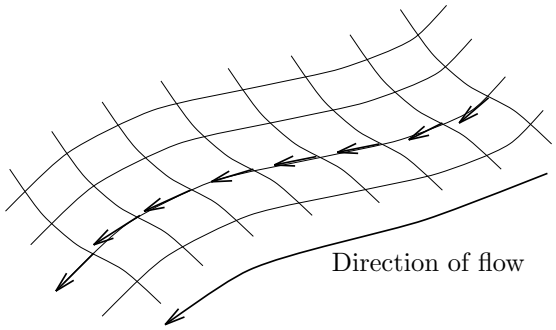

Figure 1.7: *Schematic representation of the line kinematic condition.*

defining the line kinematic condition is

$$\boldsymbol{c} - c_\tau \boldsymbol{\tau} = \boldsymbol{0}, \tag{1.39}$$

where $\boldsymbol{c}$ is a quantity closely related to the fluid velocity and c_τ is its component tangential to the line ($c_\tau = \boldsymbol{c} \cdot \boldsymbol{\tau}$). Note that $\boldsymbol{\tau}$, and thus c_τ are functions of the nodal coordinates on the line. Thus equation (1.39) involves the coordinates as unknowns.

An interesting feature of the line kinematic condition is that it allows the use of a continuation method on a parameter ζ_l. This allows to progressively model the kinematic condition. This is done by calculating vector $\boldsymbol{c}$ with

$$\boldsymbol{c} = \zeta_l \boldsymbol{v} + (1 - \zeta_l)||\boldsymbol{v}||\boldsymbol{\tau}_{\text{ref}}, \tag{1.40}$$

in which $\boldsymbol{v}$ is the fluid velocity, and $\boldsymbol{\tau}_{\text{ref}}$ is a reference vector tangential to the initial mesh line. By putting ζ_l to 0, $\boldsymbol{c}$ remains parallel to the initial mesh line, and the line does not move. By progressively increasing ζ_l, the kinematic condition is introduced in the equation. for $\zeta_l = 1$ the full kinematic condition is obtained.

1.5.2 Surface tension

Along a free surface, the modelling of surface tension leads to a normal force applied on the interface:

$$\boldsymbol{f}_n = \gamma \left(\frac{1}{R_1} + \frac{1}{R_2} \right) \boldsymbol{n}, \tag{1.41}$$

in which $\boldsymbol{n}$ is the normal vector to the surface, R_1 and R_2 are the principal radii of curvature of the surface, and γ is the surface tension coefficient. For an

axisymmetric flow around x axis, the principal radii of curvature are given by

$$R_1 = \left[1 + \left(\frac{\partial h}{\partial x}\right)^2\right]^{\frac{3}{2}} \Big/ \frac{\partial^2 h}{\partial x^2},$$
$$R_2 = -h\left[1 + \left(\frac{\partial h}{\partial x}\right)^2\right]^{\frac{1}{2}}.$$

For a planar flow, the formula giving R_1 remains unchanged and R_2 becomes infinite.

After discretization and integration by parts of equation (1.41), two different types of boundary conditions may be imposed to the free surface: Dirichlet or Neumann boudary conditions. In some case, the attachment position of the free surface on the wall is known a priori. This is the case when the free surface attaches to a corner. For such cases, Dirichlet conditions are imposed. In other cases, the attachment point is the result of a dynamic equilibrium of contact forces. For such situations, one usually imposes a force equal to surface tension and oriented towards a specified direction (Figure 1.8). Such problems are discussed in [Rus80, Keu86, Leg92].

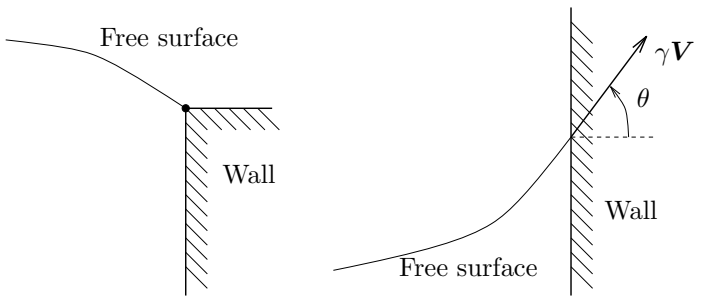

Figure 1.8: *Different types of boundary conditions that may be imposed at the attachment point of the free surface and a wall.*

Note that it is often easier to derive the discretized equations of surface tension from a minimization principle, the function to minimize being the energy associated with the total free surface: $E = \gamma S$.

1.5.3 Remeshing techniques

In order to avoid overdistortion of elements, a remeshing technique is used to propagate the motion of the free surface into the mesh. In this section we only mention the method of spines, a remeshing based on a Thompson transformation and a remeshing based on the minimization of the deformation energy of a grid (called Optimesh in Polyflow).

Method of spines

Let us first define a height function $h(x,t)$ representing the displacement of free surface nodes towards a specified direction $\boldsymbol{d}$. The kinematic condition may be expressed as a function of h. In the method of spines, a one dimensional finite element approximation is constructed for the height function h on the free surface (Figure 1.9). We only present the method here for two-dimensional calculations, but it is easy to generalize the calculation to three-dimensional flows.

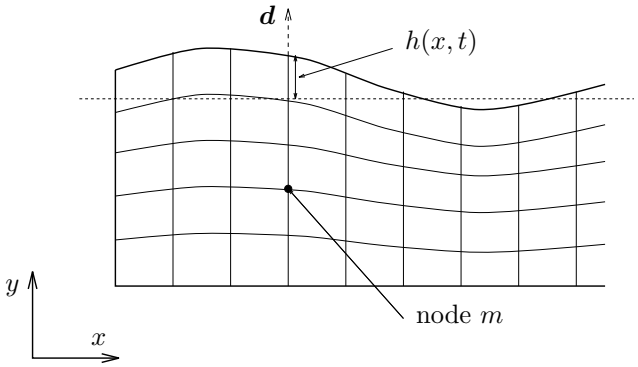

Figure 1.9: *Schematic representation of the method of spines.*

The mesh is then divided into "slices". In a given slice, the nodal displacement of each node is a linear function of the nodal displacement of the free surface node of that slice. It may thus be expressed as a function of h:

$$\Delta \boldsymbol{x}_{mn}(t) = c_{mn} h_m(t) \boldsymbol{d}_m, \tag{1.42}$$

in which m is a nodal index in the horizontal direction of slicing, m is a nodal index in the vertical direction, and c_{mn} is a constant parameter related to the initial position of the node (m,n) in the undeformed mesh.

In general, $\boldsymbol{d}_m$ may be updated at each time step (or continuation step). For example, the vector may be calculated at the beginning of each time step in order to have it normal to the mesh before any other calculation. But $\boldsymbol{d}_m$ may also be determined only once at the beginning of the calculation; that is what we are doing in chapter 2 where director vector $\boldsymbol{d}$ is vertical or horizontal.

Note that an interesting advantage of the method of spines is that each coordinate unknown is a linear function of one single variable $h_m(t)$. Thus equation (1.42) may be expressed with constraints. This leads to an important decrease of the computational cost of the remeshing for coordinate unknowns are eliminated of the system before the Gaussian elimination. Therefore, the method of spines is a very cheap remeshing technique. But its use is limited to problems in which the deformation of the mesh is not too large.

Remeshing based on a Thompson transformation

When we use the Thompson transformation, we take advantage of the smoothing properties of an elliptic operator [TWM85, TWM82]. As a first step, a generalised coordinate system is defined on the moving domain. For a two-dimensional domain, one builds a mapping between the two-dimensional domain and a "parent element". In Polyflow the use of Thompson remeshing is limited to problems in which the domain to remesh as a quadrilateral topology, and the parent element is square.

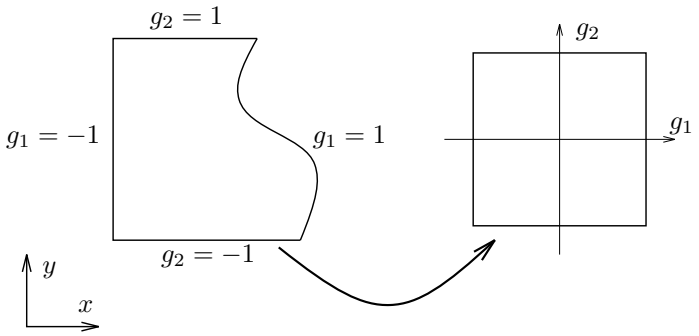

Figure 1.10: *Schematic representation of the mapping between the domain to remesh and the square parent element for the Thompson transformation.*

The mapping is obtained by solving

$$\nabla^2 \boldsymbol{g} = \mathbf{0},$$

in which $\boldsymbol{g}$ is a vectorial function $\{g_1, g_2\}^{\mathrm{T}}$ of the coordinates. For that problem, Dirichlet boundary conditions are imposed on the components of $\boldsymbol{g}$. Those conditions are indicated in Figure 1.10. The components of $\boldsymbol{g}$ may be interpreted as generalised coordinates. In Figure 1.10, they are such that the parent element is a square centered on the origin, and of side length 2.

The field $\boldsymbol{g}$ contains information on the initial distribution of the elements in the domain. This information is used to calculate the motion of the nodes when the boundaries of the domain move. More precisely, we solve

$$\nabla^2 \boldsymbol{g} = \mathbf{0},$$

but here, the field $\boldsymbol{g}$ is a data of the problem, and the coordinates are the unknowns. Thus we search $\{x, y\}^{\mathrm{T}}$ such that relation $\nabla^2 \boldsymbol{g} = \mathbf{0}$ is conserved. This leads to a nonlinear set of equations with coordinate as unknowns. This set of equations is solved with a Newton-Raphson algorithm. The equations involving the nodal coordinates along the boundaries are cancelled and replaced by essential boundary conditions (fixed coordinates), or tangential Thompson remeshing and kinematic conditions, or any other equation depending on the pecularity of the problem being solved.

The main advantage of the Thompson remeshing resides in the fact that the elliptic operator has smoothing properties on the deformation of the mesh. This allows very large deformations. But the computational cost of the method also is larger than that of the method of spines.

Remeshing based on an energetic approach

In the "Optimesh" remeshing technique of Polyflow, the mesh is considered as a deforming elastic grid. An elastic response corresponds to the angular deformation of the corners, of the diagonal of elements, and of the side of elements. An energy may be associated with the deformation of the grid, and the remeshing is the result of the minimization of that energy: one solves an elastic problem.

Some parameters allow the user to modify the contribution of the various elements of the elastic response (angular, diagonal or side deformations). It is also possible to consider the initial grid as a reference for the elastic deformations.

More details about this remeshing technique may be found in [Ber91].

1.5.4 Correction for time derivatives

Special care must be taken in the evaluation of time derivatives when the Galerkin procedure is used on a moving grid algorithm. For example, the material derivative of the extra-stress tensor becomes

$$\frac{D\boldsymbol{T}}{Dt} = \dot{\boldsymbol{T}} + (\boldsymbol{v} - \dot{\boldsymbol{x}}) \cdot \nabla \boldsymbol{T}.$$

If the discretization is done on a fixed mesh, $\dot{\boldsymbol{x}} = \boldsymbol{0}$, and the material derivative reduces to its usual expression. Another special case corresponds to the Lagrangian approach in which nodes are fluid particles and $\boldsymbol{v} = \dot{\boldsymbol{x}}$. In that case the material derivative reduces to the time derivative [Keu86].

Part I

Numerical calculation of multilayer flows

Part II

Numerical calculation of extensional flows

Part III

Appendices

Bibliography

[AH94] J. Azaiez and G. M. Homsy. *Journal of Non-Newtonian Fluid Mechanics*, 54:333, 1994. 33

[APW90] N. R. Anturkar, T. C. Papanastasiou, and J. O. Wilkes. Linear Stability Analysis of Multilayer Plane Poiseuille Flow. *Phys. Fluids*, A2(4):530–541, 1990. 56

[BC94] C. Bodart and M. J. Crochet. The time-dependent flow of a viscoelastic fluid around a sphere. *Journal of Non-Newtonian Fluid Mechanics*, 54:303–329, 1994. 199

[BCAH87] R. B. Bird, C. F. Curtiss, R. C. Armstrong, and Ole Hassager. *Dynamics of Polymeric liquids*, volume 2 Kinetic Theory. John Wiley & Sons, 1987. 21, 175

[BCJ92] R. Bai, K. Chen, and D. D. Joseph. Lubricated Pipelining V: Stability of Core-Annular Flow. Experiments and comparison with theory. *J. Fluid Mech.*, ???:???, 1992. 81, 83, 86, 89

[BDJ80] R. B. Bird, P. J. Dotson, and N. L. Johnson. Polymer solution rheology based on a finitely extensible bead-spring chain model. *Journal of Non-Newtonian Fluid Mechanics*, 7:213–235, 1980. 33

[Ber91] D. Berghezan. *Simulation numérique d'écoulements en couches intervenant dans l'industrie photographique*. PhD thesis, Université Catholique de Louvain, 1991. 46

[BH82] A. N. Brooks and T. J. R. Hughes. Streamline Upwind/Petrov-Galerkin Formulations for Convection Dominated Flows with Particular Emphasis on the Incompressible Navier-Stokes Equations. *Computer Methods in Applied Mechanics and Engineering*, 32:199–259, 1982. 38

[BHAC77] R. B. Bird, O. Hassager, R. C. Armstrong, and C. F. Curtiss. *Dynamics of Polymeric liquids*, volume 2 Kinetic Theory. John Wiley & Sons, 1977. 21, 28, 29

[BM84] J. W. Barret and K. W. Morton. Approximate Symmetrization and Petrov-Galerkin Methods for Diffusion-Convection Problems. *Computer Methods in Applied Mechanics and Engineering*, 45:97–122, 1984.

[BM92] P. A. M. Boomkamp and R. H. M. Miesen. Nonaxisymmetric waves in core-annular flow with a small viscosity ratio. *Phys. Fluids A*, 4(8):1627–1636, 1992.

[Bod94] C. Bodart. *Ecoulements Viscoélastiques transitoires et Sédimentation*. PhD thesis, Université Catholique de Louvain, décembre 1994. 21, 199, 201

[Bre74] F. Brezzi. On the existence, Uniqueness and Approximation of Saddle-point Problem Arising from Lagrange Multipliers. *Revue Française 'Automatique Inform. Rech. Opér., Série Rouge Anal. Numér.*, R-2:129–151, 1974. 35

[BS78] A. J. Baker and M. O. Soliman. Utility of a Finite Element Solution Algorithm for Initial-Value Problems. *Journal of Computational Physics*, 32:289–324, 1978.

[CAD+95a] J. A. Covas, J. F. Agassant, A. C. Diogo, J. Vlachopoulos, and K. Walters, editors. *Rheological Fundamentals of Polymer Processing*, volume 302 of *NATO ASI Series*. Kluwer Academic Publishers, 1995. 21, 39

[CAD+95b] J. A. Covas, J. F. Agassant, A. C. Diogo, J. Vlachopoulos, and K. Walters, editors. *Rheological Fundamentals of Polymer Processing*, volume 302 of *NATO ASI Series*, pages 265–288. Kluwer Academic Publishers, 1995. 49, 50, 100, 102

[Cas96] B. Caswell. Report on the IXth International Workshop on Numerical Methods in Non-Newtonian Flows. *Journal of Non-Newtonian Fluid Mechanics*, 62:99–110, 1996. 147, 149

[CBJ90] K. Chen, R. Bai, and D. D. Joseph. Lubricated Pipelining III: Stability of Core-Annular Flow in Vertical Pipes. *J. Fluid Mech.*, 214:251–286, 1990. 81, 83, 86

[CGH61] M. E. Charles, G. W. Govier, and G. W. Hodgson. The Horizontal Pipeline Flow of Equal Density of Oil-Water Mixtures. *The Canadian Journal of Chemical Engineering*, 39:17–36, 1961. 81, 86, 87

[CGMZ76] I. Christie, D. F. Griffiths, A. R. Mitchell, and 0. C. Zienkiewicz. Finite Element Methods for Second Order Differential Equations with Significant First Derivatives. *International Journal for Numerical Methods in Engineering*, 10:1389–1396, 1976.

[CJ88] G. F. Carey and B. N. Jiang. Least-Squares Finite Elements for First-Order Hyperbolic Systems. *International Journal for Numerical Methods in Engineering*, 26:81–93, 1988.

[CJ91a] K. Chen and D. D. Joseph. Long wave and lubrication theories for core-annular flows. *Phys. Fluids A*, 3(11):2672, 1991.

[CJ91b] K. Chen and D. D. Joseph. Lubricated Pipelining IV: Stability of Core-Annular Flow: Guinzburg-Landau equations. *J. Fluid Mech.*, 227:587, 1991.

[CK80] M. J. Crochet and R. Keunings. Die Swell of a Maxwell Fluid: Numerical Prediction. *Journal of Non-Newtonian Fluid Mechanics*, 7:199–212, 1980. 35

[CM79] M. J. P. Cullen and K. W. Morton. Analysis of Evolutionary Error in Finite Element and Other Methods. *Journal of Computational Physics*, 34:245–267, 1979.

[Cou94] W. Couzy. Higher-order splitting methods for the discretized Navier-Stokes equations. *CESAME-UCL*, 1994.

[CR88] M. D. Chilcott and J. N. Rallison. Creeping flow of dilute polymer solutions past cylinders and spheres. *Journal of Non-Newtonian Fluid Mechanics*, 29:381–432, 1988. 33, 151

[CTW93] E. O. A. Carew, P. Townsend, and M. F. Webster. A Taylor-Petrov-Galerkin Algorithm for Viscoelastic Flow. *Journal of Non-Newtonian Fluid Mechanics*, 50:253–287, 1993.

[DADH97] B. Debbaut, T. Avalosse, J. Dooley, and K. Hughes. On the development of secondary motions in straight channels induced by the second normal stress difference: experiments and simulations. *Journal of Non Newtonian Fluid Mechanics*, 69:255–271, 1997. 139

[DC87] J. Dheur and M. J. Crochet. Newtonian stratified flow through an abrupt expansion. *Rheologica Acta*, 26:401–413, 1987. 118

[DC88] B. Debbaut and M. J. Crochet. Extensional effects in complex flows. *Journal of Non-Newtonian Fluid Mechanics*, 30:169–184, 1988. 147

[DG84] D. B. Duncan and D. F. Griffiths. The Study of a Petrov-Galerkin Method for First-Order Hyperbolic Equations. *Computer Methods in Applied Mechanics and Engineering*, 45:147–166, 1984.

[DGL82] J. Donea, S. Giuliani, and H. Laval. Finite Element Solution of the Unsteady Navier-Stokes Equation by a Fractional Step Method. *Computer Methods in Applied Mechanics and Engineering*, 30:53–73, 1982.

[DGLQ84] J. Donea, S. Giuliani, H. Laval, and L. Quartapelle. Time-Accurate Solution of Advection-Diffusion Problems by Finite Elements. *Computer Methods in Applied Mechanics and Engineering*, 45:123–145, 1984.

[DQS87] J. Donea, L. Quartapelle, and V. Selmin. An analysis of Time Discretization in the Finite Element Solution of Hyperbolic Problems. *Journal of Computational Physics*, 70:463–499, 1987.

[DS97] P. S. Doyle and E. S. G. Shaqfeh. Dynamic Simulation of Freely-Draining, Flexible Bead-Rod Chains: Start-up of Extensional and Shear Flow. *Submitted to the Journal of Non-Newtonian Fluid Mechanics*, June 1997. 147, 173, 184

[DSMS97] P. S. Doyle, E. S. G. Shaqfeh, G. H. McKinley, and S. H. Spiegelberg. Relaxation of Dilute Polymer Solutions Following Extensional Flow. *Submitted to the Journal of Non-Newtonian Fluid Mechanics*, June 1997. 147, 173, 184

[DW84] T. F. Dupont and L. B. Wahlbin. An Analysis of Dendy's Piecewise Polynomial Petrov-Galerkin Method for a Hyperbolic Equation with Stagnation Points. *Computer Methods in Applied Mechanics and Engineering*, 45:165–175, 1984.

[Eve73] A. E. Everage. Theory of Stratified Bicomponent Flow of Polymer Melts. I. Equilibrium Newtonian Tube Flow. *Transactions of the Society of Rheology*, 17:629–646, 1973. 99

[Eve75] A. E. Everage. Theory of Stratified Bicomponent Flow of Polymer Melts. II. Interface Motion in Transient Flows. *Transactions of the Society of Rheology*, 19:509–522, 1975. 49, 99, 100, 101

[FBL+87] A. L. Frenkel, A. J. Babchin, B. G. Levich, T. Shlang, and G. I. Sivashinsky. Annular flows can keep unstable films from breakup: nonlinear saturation of capillary instability. *J. Colloid. Interface Sci.*, 115:225–233, 1987.

[For81] M. Fortin. Old and New Finite Elements for Incompressible Flows. *International Journal for Numerical Methods in Fluids*, 1:347–364, 1981. 38, 118

[GCLU84a] P. N. Gresho, S. T. Chan, R. L. Lee, and C. D. Upson. A Modified Finite Element Method for Solving the Time-Dependent Incompressible Navier-Stokes Equations. Part 1: Theory. *International Journal for Numerical Methods in Fluids*, 4:557–598, 1984.

[GCLU84b] P. N. Gresho, S. T. Chan, R. L. Lee, and C. D. Upson. A Modified Finite Element Method for Solving the Time-Dependent Incompressible Navier-Stokes Equations. Part 2: Applications. *International Journal for Numerical Methods in Fluids*, 4:619–640, 1984.

[GF95] R. Guénette and M. Fortin. A new mixed finite element method for computing viscoelastic flows. *Journal of Non-Newtonian Fluid Mechanics*, 60(1):27–52, 1995. 37

[GLS80] P. M. Gresho, R. L. Lee, and R. L. Sani. *Recent Advances in Numerical Methods in Fluids*, volume 1, chapter 2 On the Time dependent Solution of the Incompressible Navier-Stokes Equations in two or three Dimensions, pages 27–80. Pineridge, Swansea, 1980. 199

[GNOZ82] R. H. Gallagher, D. H. Norrie, J. T. Oden, and O. C. Zienkiewicz. *Finite Elements in Fluids*, volume 4. John Wiley and sons, 1982.

[GS87] P. M. Gresho and R. L. Sani. On Pressure Boundary Conditions for the Incompressible Navier-Stokes Equations. *International Journal for Numerical Methods in Fluids*, 7:1111–1145, 1987.

[Han73] Chang Dae Han. A Study of Bicomponent Coextrusion of Molten Polymers. *Journal of Applied Polymer Science*, 17:1289–1303, 1973. 99, 110, 111, 132, 138, 141, 143

[HB83] A. P. Hooper and W. G. C. Boyd. Shear-Flow Instability at the Interface Between two Viscous Fluids. *J. Fluid Mech.*, 128:507–528, 1983. 57, 84

[HB87] A. P. Hooper and W. G. C. Boyd. Shear-Flow Instability Due to a Wall and a Viscosity Discontinuity at the Interface. *J. Fluid Mech.*, 179:201–225, 1987. 53, 56, 57

[HG85] A. P. Hooper and R. Grimshaw. Nonlinear instability at the interface between two viscous fluids. *Phys. Fluids*, 28:37–45, 1985.

[Hic71] C. E. Hickox. Instability Due to Viscosity and Density Stratification in Axisymmetric Pipe Flow. *Phys. Fluids*, 14:251–262, 1971. 84

[HJ90] H. H. Hu and D. D. Joseph. Lubricated Pipelining II: Stability of Core-Annular Flows. *J. Fluid Mech.*, 205:358–396, 1990.

[HK76a] C. D. Han and Y. W. Kim. Further Onservations of the Interface of Conjugate Fibers. *Journal of Applied Polymer Science*, 20:2609–2614, 1976. 102, 110

[HK76b] C. D. Han and Y. W. Kim. Use of the Coextrusion Technique for Producing Flame-Retardant and Antistatic Fibers. *Journal of Applied Polymer Science*, 20:2913–2918, 1976. 102

[HK81] J. P. Huffenus and D. Khaletzky. The Lagrangien Approach of Advective Term Treatment and its Application to the Solution of Navier-Stokes Equations. *International Journal for Numerical Methods in Fluids*, 1:365–387, 1981.

[HLB79] T. J. R. Hughes, W. K. Liu, and A. Brooks. Finite Element Analysis of Incompressible Viscous Flows by the Penalty Function Formulation. *Journal of Computational Physics*, 30:1–60, 1979.

[HLZ81] T. J. R. Hughes, W. K. Liu, and T. K. Zimmermann. Lagrangian-Eulerian Finite Element Formulation for Incompressible Viscous Flows. *Computer Methods in Applied Mechanics and Engineering*, 29:329–349, 1981.

[HMM86] T. J. R. Hughes, M. Mallet, and A. Mizukami. A New Finite Element Formulation for Computational Fluid Dynamics: II. Beyond SUPG. *Computer Methods in Applied Mechanics and Engineering*, 54:341–355, 1986.

[HMN70] D. Hasson, U. Mann, and A. Nir. Annular Flow of Two Immiscible Liquids I: Mechanisms. *The Canadian Journal of Chemical Engineering*, 48:514–520, 1970.

[Hoo85] A. P. Hooper. Long-Wave Instability at the Interface Between Two Viscous Fluids: Thin Layer Effects. *Phys. Fluids*, 28(5):1613–1618, 1985. 56

[Hoo89] A. P. Hooper. The stability of two superposed viscous fluids in a channel. *Phys. Fluids A*, 1(7):1133–1142, 1989. 56

[HPP86] I. I. Hesla, F. R. Pranckh, and L. Preziosi. Squire's Theorem for two Stratified Fluids. *Phys. Fluids*, 29(9):2808–2811, 1986.

[HPT79] T. J. R. Hughes, K. S. Pister, and R. L. Taylor. Implicit-Explicit Finite Elements in Nonlinear Transient Analysis. *Computer Methods in Applied Mechanics and Engineering*, 17/18:159–182, 1979.

[HTJTW90] D. M. Hawken, H. R. Tamaddon-Jahromi, P. Townsend, and M. F. Webster. A Taylor-Galerkin-Based Algorithm for Viscous Incompressible Flow. *International Journal for Numerical Methods in Fluids*, 10:327–351, 1990.

[Hug78] T. J. R. Hughes. A Simple Scheme for Developing 'Upwind' Finite Elements. *International Journal for Numerical Methods in Engineering*, 12:1359–1365, 1978.

[Hug87] T. J. R. Hughes. Recent Progress in the Development and Understanding of SUPG Methods with Special Reference to the Compressible Euler and Navier-Stokes Equations. *International Journal for Numerical Methods in Fluids*, 7:1261–1275, 1987.

[JC88] B. N. Jiang and G. F. Carey. A Stable Least-Squares Finite Element Method for Non-Linear Hyperbolic Problems. *International Journal for Numerical Methods in Fluids*, 8:933–942, 1988.

[JNP84] C. Johnson, U. Nävert, and J. Pitkäranta. Finite Element Methods for Linear Hyperbolic Problems. *Computer Methods in Applied Mechanics and Engineering*, 45:285–312, 1984.

[JR93a] D. D. Joseph and Y. Y. Renardy. *Fundamentals of Two Fluids Dynamics. Part I: Mathematical Theory and Applications*. Springer-Verlag, 1993. 49, 55

[JR93b] D. D. Joseph and Y. Y. Renardy. *Fundamentals of Two Fluids Dynamics. Part II: Lubricated Pipelining and Immiscible Liquids*. Springer-Verlag, 1993. 49, 81, 83, 86, 89

[JRR84] D. D. Joseph, M. Renardy, and Y. Renardy. Instabilities of the Flow of two Immiscible Liquids with Different Viscosities in a Pipe. *J. Fluid Mech.*, 141:309–317, 1984. 84

[Keu86] R. Keunings. An algorithm for the simulation of transient viscoelastic flows with free surfaces. *Journal of Computational Physics*, 62:199–220, 1986. 43, 46

[Keu89] R. Keunings. Simulation of viscoelastic fluid flow. In C.L. Tucker III, editor, *Fundamentals of Computer Modeling for Polymer Processing*, pages 403–470. Carl Hanser Verlag, 1989. 36

[KH76] A. A. Khan and C. D. Han. On the Interface Deformation in the Stratified Two-Phase Flow of Viscoelastic Fluids. *Transactions of the Society of Rheology*, 20:595–621, 1976. 100, 102

[Kho90a] B. Khomami. Interfacial Stability and Deformation of Two Stratified Power Law Fluids in Plane Poiseuille Flow. Part I. Stability Analysis. *Journal of Non-Newtonian Fluid Mechanics*, 36:289–303, 1990.

[Kho90b] B. Khomami. Interfacial Stability and Deformation of Two Stratified Power Law Fluids in Plane Poiseuille Flow. Part II. Interface Deformation. *Journal of Non-Newtonian Fluid Mechanics*, 37:19–36, 1990.

[KHV90] A. Karagiannis, A. N. Hrymak, and J. Vlachopoulos. Three dimensional studies on bicomponent extrusion. *Rheologica Acta*, 29:71–87, 1990. 100, 101, 102, 123

[Kra44] H. A. Kramers. *Physica*, 11:1, 1944. 31

[KT77] M. Kawahara and N Takeuchi. Mixed Finite Element Method for Analysis of Viscoelastic Fluid Flow. *Computers and Fluids*, 5:33–45, 1977. 35

[L$\ddot{\text{o}}$89] R. Löhner. Adaptative Remeshing for Transient Problems. *Computer Methods in Applied Mechanics and Engineering*, 75:195–214, 1989.

[Lar88] R. G. Larson. *Constitutive Equations for Polymer Melts and Solutions*. Butterworths:Boston, 1988. 21, 28

[Leg92] V. Legat. *Méthodes d'éléments finis pour le calcul d'écoulements tridimensionnels à surfaces libres*. PhD thesis, 1992. ix, 21, 43, 198, 212

[LHJ+97] G. Lielens, P. Halin, I. Jaumain, R. Keunings, and V. Legat. New closure approximations for the kinetic theory of finitely extensible dumbbells,. *J. Non-Newtonian Fluid Mech.*, in press 1997. 147, 187, 189, 191, 193

[LKLon] G. Lielens, R. Keunings, and V. Legat. Evaluation of the FENE-L model in three-dimensional flow fields,. in preparation. 147, 189, 191

[LMZ84] R. Löhner, K. Morgan, and O. C. Zienkiewicz. The Solution of Non-Linear Hyperbolic Equation Systems by the Finite Element Method. *International Journal for Numerical Methods in Fluids*, 4:1043–1063, 1984.

[LQ91] H. Laval and L. Quartapelle. A Fractional-Step Taylor-Galerkin Method for Unsteady Incompressible Flows. *International Journal for Numerical Methods in Fluids*, 11:501–513, 1991.

[LW74] B. L. Lee and J. L. White. An experimental Study of Rheological Properties of Polymer Melts in Laminar Shear Flow and of Interface Deformation and Its Mechanisms in Two-Phase Stratified Flow. *Transactions of the Society of Rheology*, 18:467–492, 1974. 99, 102

[Mac94] C. W. Macosko. *Rheology: Principles, Measurements and Applications*. VCH Publishers, 1994. 21, 25

[MBD+92] R. Miesen, G. Beijnon, P. E. M. Duijvestijn, R. V. A. Oliemans, and T. Verheggen. Interfacial waves in core-annular flow. *J. Fluid Mech.*, 238:97–117, 1992. 81

[MC86] J. M. Marchal and M. J. Crochet. Hermitian Finite Element for Calculating Viscoelastic Flow. *Journal of Non-Newtonian Fluid Mechanics*, 20:187–207, 1986. 36

[MC87] J. M. Marchal and M. J. Crochet. A new mixed finite element for calculating viscoelastic flow. *Journal of Non-Newtonian Fluid Mechanics*, 26:77–114, 1987. 36, 147

[McK95] G. H. McKinley. Steady and transient motion of a sphere sedimenting through shear-thinning and constant-viscosity elastic fluids. *BSR Annual Award Lecture, IXth International Workshop on Numerical Methods in Non-Newtonian Flows*, 1995. 149, 153, 154, 166

[Miz94] A. Mizukami. Element by element penalty/Uzawa formulation for large scale flow problems. *Computer Methods in Applied Mechanics and Engineering*, 112:283–289, 1994.

[Mor85] K. W. Morton. Generalised Galerkin Methods for Hyperbolic Problems. *Computer Methods in Applied Mechanics and Engineering*, 52:847–871, 1985.

[MP80] K. W. Morton and A. K. Parrot. Generalised Galerkin Methods for First-Order Hyperbolic Equations. *Journal of Computational Physics*, 36:249–270, 1980.

[Old50] J. G. Oldroyd. *Proceedings of the Royal Society*, A200:523, 1950. 25

[OS94] Y. W. Ooi and T. Sridhar. Extensional rheometry of fluid S1. *Journal of Non-Newtonian Fluid Mechanics*, 52:153–162, 1994. 147, 180

[OS96] N. V. Orr and T. Sridhar. Stress relaxation in uniaxial extension. *Journal of Non-Newtonian Fluid Mechanics*, 67:77–103, 1996. 147, 173, 178, 179, 180

[P. 62] P. D. Lax and B. Wendroff. On the stability of difference schemes. *Communication in Pure Applied Mathematics*, 15:363, 1962.

[PCa] B. Purnode and M. J. Crochet. Flows of polymer solution through contractions, part I: Flows of polyacrylamide solutions through planar contractions. *to be published in Journal of Non-Newtonian Fluid Mechanics*. 191

[PCb] B. Purnode and M. J. Crochet. Flows of polymer solution through contractions, part II: Flows of fluid M1 through axisymmetric contractions. *to be published in Journal of Non-Newtonian Fluid Mechanics*. 147, 191

[PCc] B. Purnode and M. J. Crochet. Polymer solution characterization with the FENE-P model. *to be published in Journal of Non-Newtonian Fluid Mechanics*. 147

[PCJ89] L. Preziosi, K. Chen, and D. D. Joseph. Lubricated pipelining I: stability of core-annular flow. *J. Fluid Mech.*, 201:323–356, 1989. 82, 83, 85, 86, 87, 88

[Pea85] A. J. Pearlstein. On the Two-Dimensionality of the Critical Disturbances for Stratified Viscous Plane Parallel Shear Flows. *Phys. Fluids*, 28:751, 1985.

[Per93] J. B. Perot. An analysis of the Fractional Step Method. *Journal of Computational Physics*, 108:51–58, 1993.

[Pet66] A. Peterlin. *Journal of Polymer Science, Polymer Letters*, 4B:287, 1966. 32

[PMR90] D. T. Papageorgiou, C. Maldarelli, and D. S. Rumschitzki. Nonlinear interfacial stability of core annular film-flows. *Phys. Fluids*, A2:340–352, 1990.

[PN95] J. Petera and V. Nassehi. Use of the finite element modelling for the improvement of viscometry results obtained by cone-and-plate rheometers. *Journal of Non-Newtonian Fluid Mechanics*, 58:1–24, 1995. 147

[Pur96] B. Purnode. *Vortices and Change of Type in Contraction Flows of Viscoelastic Fluids*. PhD thesis, Université Catholique de Louvain, february 1996. 21, 29

[Ray79] Lord Rayleigh. On the instability of jets. *Proc. Roy. London. Math. Soc.*, 10:4, 1879.

[RBA90] D. Rajagopalan, R.A. Brown, and R.C. Armstrong. Finite element methods for calculations of steady viscoelastic flow using constitutive equations with a Newtonian viscosity. *Journal of Non-Newtonian Fluid Mechanics*, 36:159–192, 1990. 37

[Ren88] Y. Renardy. Stability of the Interface in Two-Layer Couette Flow of Upper Convected Maxwell Liquids. *Journal of Non-Newtonian Fluid Mechanics*, 282:359–375, 1988.

[Rou53] P. E. Rouse. *Journal of Chemical Physics*, 21:1272, 1953. 29, 175

[RS85] J. G. Rice and R. J. Schnipke. A Monotone Streamline Upwind Finite Element Method for Convection-Dominated Flows. *Computer Methods in Applied Mechanics and Engineering*, 48:313–327, 1985.

[Rus80] K. J. Ruschak. A method for incorporating free boundaries with surface tension in finite element fluid flow simulators. *International Journal for Numerical Methods in Engineering*, 15:639–648, 1980. 43

[SAM96] S. H. Spiegelberg, D. C. Ables, and G. H. McKinley. The role of end effects on measurements of extensional viscosity in filament stretching rheometers. *Journal of Non-Newtonian Fluid Mechanics*, 64:229–267, 1996. 147, 149, 150, 158, 163, 164, 166

[SB73] J. H. Southern and R. L. Ballman. Stratified Bicomponent Flow of Polymer Melts in Tube. *Applied Polymer Science*, 20:175–189, 1973. 49, 99

[SB75] J. H. Southern and R. L. Ballman. Additional Observations on Stratified Bicomponent Flow of Polymer Melts in Tube. *Journal of Polmer Science*, 13:863–869, 1975. 49, 99

[SDK91] R. W. G. Shipman, M. M. Denn, and R. Keunings. Mechanics of the "falling plate extensional" rheometer. *Journal of Non-Newtonian Fluid Mechanics*, 40:281–288, 1991. 147

[SDQ85] V. Selmin, J. Donea, and L. Quartapelle. Finite Element Methods for Nonlinear Advection. *Computer Methods in Applied Mechanics and Engineering*, 52:817–845, 1985.

[SK92] Y.-Y. Su and B. Khomami. Interfacial Stability of Multilayer Viscoelastic Fluids in Slit and Converging Channel Die Geometries. *Journal of Rheology*, 36(2):357–387, 1992. 49

[SL97] R. Sizaire and V. Legat. Finite element simulation of a filament stretching rheometer. *Journal of Non-Newtonian Fluid Mechanics*, 71:89–107, 1997. 149

[SL98] R. Sizaire and V. Legat. Calculation of 3D encapsulation flows with the finite element method. *in preparation*, 1998. 99

[SLJ+98] R. Sizaire, G. Lielens, I. Jaumain, R. Keunings, and V. Legat. Influence of non-linearity and dispersity on the behaviour of viscoelastic fluids in rheometrical extensional flows. *in preparation*, 1998. 174, 188, 189, 190

[SM96a] M. J. Solomon and S. J. Muller. The transient extensional behavior of polystyrene-based Boger fluids of varying solvent quality and molecular weight. *Journal of Rheology*, 40:837–856, 1996. 147, 149, 163, 164, 166

[SM96b] S. H. Spiegelberg and G. H. McKinley. Stress relaxation and elastic decohesion of viscoelastic polymer solutions in extensional flows. *Journal of Non-Newtonian Fluid Mechanics*, 67:49–76, 1996. 156

[SPTT96] J. Sun, N. Phan-Thien, and R.I. Tanner. An adaptive viscoelastic stress splitting scheme and its applications: AVSS/SI and AVSS/SUPG. *Journal of Non-Newtonian Fluid Mechanics*, 65:75–91, 1996. 37

[Squ33] H. B. Squire. On the Stability of Three Dimensionnal Disturbances for Stratified Viscous Flow Between Parallel Walls. *Proc. Roy. Soc.*, A142:621, 1933.

[SS80] W. J. Silliman and L. E. Scriven. Separating Flow Near a Static Contact Line: Slip at a Wall and Shape of a Free Surface. *Journal of Computational Physics*, 34:287–313, 1980. 118, 119

[SSBF85] T. Shlang, G. I. Sivashinsky, A. J. Babchin, and A. L. Frenkel. Irregular wavy flow due to viscosity stratification. *J. Phys. Paris*, 46:863–866, 1985.

[THV+93] A. Torres, A. N. Hrymak, J. Vlachopoulos, J. Dooley, and B. T. Hilton. Boundary conditions for contact lines in coextrusion flows. *Rheologica Acta*, 32:513–525, 1993. 50, 118, 119

[TJTW92] H. R. Tamaddon-Jahromi, P. Townsend, and M. F. Webster. Numerical Solution of Unsteady Viscous Flows. *Computer Methods in Applied Mechanics and Engineering*, 95:301–315, 1992.

[TN65] C. Truesdell and W. Noll. *The Non-Linear Field Theories of Mechanics*. Springer-Verlag, 1965. 25

[Tro06] F. T. Trouton. *Proceedings of the Royal Society*, A77:426, 1906. 25

[TS93] V. Tirtaatmadja and T. Sridhar. A filament stretching device for measurement of extensional viscosity. *Journal of Rheology*, 37:1081–1102, 1993. 147, 149

[TWM82] J. F. Thompson, Z. U. A. Warsi, and C. W. Mastion. Boundary-fitted coordinate systems for numerical solutions of partial differential equations - A review. *Journal of computational physics*, 47:1, 1982. 45

[TWM85] J. F. Thompson, Z. U. A. Warsi, and C. W. Mastion. *Numerical grid generation, foundations and applications*. North-Holland, 1985. 45

[Uwa95] T. Uwaji. Studies on wrap around phenomena of stratified two phase flow. Master's thesis, Université Catholique de Louvain, October 1995. 99, 102, 123

[War96] V. Warichet. *hp-Adpativity in Finite Element Methods for Viscoelastic Flow Simulation*. PhD thesis, Université Catholique de Louvain, Novembre 1996. 21

[WH74] R. F. Warming and B. J. Hyett. The Modified Equation approach to the Stability and Accuracy Analysis of Finite-Difference Methods. *Journal of Computational Physics*, 14:159–179, 1974.

[Wil75] M. C. Williams. Migration of Two Liquid Phases in Capillary Extrusion: An Energy Interpretation. *A. I. Ch. E. Journal*, 21:1204–1207, 1975.

[WJ87] W. T. Wong and C. C. Jeng. The Stability of Two Concentric Non-Newtonian Fluids in Circular Pipe Flow. *Journal of Non-Newtonian Fluid Mechanics*, 22:359–380, 1987.

[WK93a] G. M. Wilson and B. Khomami. An Experimental Investigation of Interfacial Instabilities in Multilayer Flow of Viscoelastic Fluids. II. Elastic and Nonlinear Effects in Incompatible Polymer Systems. *Journal of Rheology*, 37(2):315–339, 1993. 49, 143

[WK93b] G. M. Wilson and B. Khomami. An Experimental Investigation of Interfacial Instabilities in Multilayer Flow of Viscoelastic Fluids. III. Compatible Polymer Systems. *Journal of Rheology*, 37(2):341–354, 1993. 49

[WOB91] L. E. Wedgewood, D. N. Ostrov, and R. B. Bird. A finitely extensible bead-spring chain model for dilute polymer solutions. *Journal of Non-Newtonian Fluid Mechanics*, 40:119–139, 1991. 173, 176

[WUDP72] J. L. White, R. C. Ufford, K. R. Dharod, and R. L. Price. Experimental and Theoretical Study of the Extrusion of Two-Phase Molten Polymer Systems. *Journal of Applied Polymer Science*, 16:1313–1330, 1972. 99, 100, 102, 103

[YH86] C. C. Yu and J. C. Heinrich. Petrov-Galerkin Methods for the Time-Dependent Convective Transport Equation. *International Journal for Numerical Methods in Engineering*, 23:883–901, 1986.

[YH87a] S. Yiantsios and B. G. Higgins. Analysis of Superposed Fluids by the Finite Element Method: Linear Stability and Flow Development. *International Journal for Numerical Methods in Fluids*, 7:247–261, 1987. 55, 56, 60, 61

[YH87b] C. C. Yu and J. C. Heinrich. Petrov-Galerkin Method for Multidimensional, Time-Dependent Convective-Diffusion Equations. *International Journal for Numerical Methods in Engineering*, 24:2201–2215, 1987.

[YH88a] S. G. Yiantsios and B. G. Higgins. . *Journal of Computational Physics*, 74:25, 1988. 55

[YH88b] S. G. Yiantsios and B. G. Higgins. Linear Stability of Plane Poiseuille Flow of Two Superposed Fluids. *Phys. Fluids*, 31(11):3225–3238, 1988. 51, 52, 55, 56, 57, 58, 59, 208

[Yih67] C.-S. Yih. Instability Due to Viscosity Stratification. *Journal of Fluid Mechanics*, 27(2):337–352, 1967. 51, 55, 56, 57

[Zie77] O. C. Zienkiewicz. *The Finite Element Method*. McGRAW-HILL, 1977.

[ZSP90] O. C. Zienkiewicz, J. Szmelter, and J. Peraire. Compressible and Incompressible Flow; an Algorithm for all Seasons. *Computer Methods in Applied Mechanics and Engineering*, 78:105–121, 1990.

[ZT89] O. C. Zienkiewicz and R. L. Taylor. *The Finite Element Method*, volume 1 Basic Formulation and Linear Problems, chapter A8, pages 605–610. McGRAW-HILL, fourth edition, 1989.

[ZT91a] O. C. Zienkiewicz and R. L. Taylor. *The Finite Element Method*, volume 2 Solid and Fluid Mechanics Dynamics and Non-linearity, chapter 12, pages 438–505. McGRAW-HILL, fourth edition, 1991.

[ZT91b] O. C. Zienkiewicz and R. L. Taylor. *The Finite Element Method*, volume 2 Solid and Fluid Mechanics Dynamics and Non-linearity, chapter 13, pages 506–556. McGRAW-HILL, fourth edition, 1991.

[ZVTN85] O. C. Zienkiewicz, J. P. Vilotte, S. Toyoshima, and S. Nakazawa. Iterative Method for Constrained and Mixed Approximation. An inexpensive Improvement of F.E.M. Performance. *Computer Methods in Applied Mechanics and Engineering*, 51:3–29, 1985.